

Anharmonicity of mixed modes and giant acoustic nonlinearity of antiferromagnetics

V. I. Ozhogin and V. L. Preobrazhenskii

I. V. Kurchatov Institute of Atomic Energy, Moscow; Institute of Radio Engineering, Electronics, and Automation, Moscow

Usp. Fiz. Nauk **155**, 593–621 (August 1988)

The results are presented of the ten-year development of the concepts of anharmonicity of the normal modes that describe the vibrations of a continuous medium having two or more mutually coupled subsystems. The results are discussed of experimental and theoretical studies of the anharmonicity of the magnetoelastic normal waves in antiferromagnetics having weak anisotropy and a large exchange field, such as α -Fe₂O₃, FeBO₃, etc. In these crystals the “effective” anharmonicity of the quasiacoustic branch of vibrations that arises from the magnetostrictive coupling of the elastic and spin subsystems is especially large—larger by a factor of 10^3 to 10^4 than that typical of a pure elastic medium. The corresponding effective moduli are controlled easily, and over a broad range, by a small magnetic field (0.1–2 kOe). The anomalously large (“giant”) magnitude of the acoustic nonlinearity has enabled observing many ultrasound analogs of the effects of nonlinear optics (frequency doubling of sound, stimulated combination scattering of sound by sound, etc.). Realization in the near future of other analogs—self-focusing of a sound wave, excitation of magnetoelastic solitons, etc., is expected.

TABLE OF CONTENTS

Introduction	713
1. Nonlinearity of mixed modes and effective anharmonicity of the elastic subsystem of a magnetic	713
2. Nonlinear magnetoelastic dynamics of antiferromagnetics with anisotropy of the “easy-plane” type	715
3. Coupled magnetoelastic waves in antiferromagnetics with anisotropy of the “easy-plane” type	717
4. Effective anharmonic elastic moduli of antiferromagnetics with anisotropy of the “easy-plane” type	718
5. Experimental nonlinear magnetoacoustics of hematite	719
6. Acoustic nonlinearity near a spin reorientation	724
7. On the quantum theory of nonlinear interactions of coupled excitations	725
8. Beyond the anharmonic approximations	726
9. Conclusion	728
References	728

INTRODUCTION

As a rule, elementary excitations of differing physical nature that exist in a solid interact with each other. Whenever the interaction leads to a linear coupling of the excitations, they are realized in crystals in the form of mixed normal modes. The set of studies of coupled excitations in a solid, encompassing primarily the problems of the formation of their “linear” characteristics (spectra, relaxation times, coupling parameters) has considerably expanded in the past decade into the field of nonlinear wave processes. Here a number of unexpectedly strong nonlinear effects have been predicted and discovered experimentally. The present article aims to call the reader’s attention to certain sharply marked and *very general* features of the formation of the nonlinear properties of a crystal due to the coupling of elementary excitations with one another, and to illustrate these features with the example of the interaction of the vibrations of a crystal lattice with the system of ordered spins of a magnetic. The objects to be examined here (nonconducting antiferromagnetics) are of independent interest—for nonlinear solid-state acoustics and for applications in the field of functional radioelectronics.

1. NONLINEARITY OF MIXED MODES AND EFFECTIVE ANHARMONICITY OF THE ELASTIC SUBSYSTEM OF A MAGNETIC

Practically any real physical systems with large enough amplitudes of some particular excitations manifest nonlinear properties. The characteristic scale that enables one to consider an amplitude to be “large” depends on the physical nature and the individual features of the interactions in the system. In crystal-lattice dynamics the natural scale for the amplitude of displacement of the nodes is the interatomic distance $a_0 \sim 3 \text{ \AA}$. In nonlinear optics the scale for the amplitude of the electric field of an electromagnetic wave is determined by the intensity of the intracrystalline electric fields $E_0 \sim e/a_0^2 \sim 10^9 \text{ V/cm}$. In the dynamics of the spin system of a magnetically ordered crystal the role of the scale for the amplitude of oscillations of the magnetization $\Delta \mathbf{M} = \mathbf{M} - \mathbf{M}_S$ is played by the magnitude of the equilibrium saturation magnetization $\mathbf{M}_S \sim \mu_B/a_0^3 \sim 10^3 \text{ G}$.

Smallness of the amplitude of an excitation as compared with the characteristic scale is the necessary condition for the approximation of the so-called weak nonlinearity and for applicability of anharmonic approximations to describe

nonlinear processes. For lattice dynamics this condition implies the requirement of small deformations $|\hat{u}| \ll 1$. When it is satisfied one can represent the density of potential energy F_e of the deformed crystal as a power series in the components of the deformation tensor \hat{u} :

$$F_e = \frac{1}{2!} \hat{C}^{(2)} \hat{u} \hat{u} + \frac{1}{3!} \hat{C}^{(3)} \hat{u} \hat{u} \hat{u} + \dots$$

The admissibility of this representation is justified both by the smallness of the attainable deformations and by the relatively weak variation in the magnitude of the anharmonic moduli as they increase in order¹: $C^{(n+1)} / C^{(n)} \sim 1-10$. This relationship of constants agrees with the existing predictions on the mechanisms of interionic interactions in crystals with different types of bonding. The upper bound of the region of applicability of the anharmonic expansion corresponds to a characteristic density of excitation energy of the order of 10^{10} erg/cm³, since $C^2 \sim 10^{12}$ erg/cm³. Under the conditions of acoustic experimentation the deformations are generally so small that usually the nonlinearity of the elastic waves can be considered weak ($|\hat{C}^{(3)} \hat{u}| / |\hat{C}^{(2)}| \ll 1$). On the contrary, in the spin systems of magnetics the conditions of strong nonlinearity are realized relatively easily. Rotation of the magnetization by large angles ($\phi \sim |\Delta M| / M_S \sim 1$) with respect to the equilibrium direction requires not very significant expenditures of energy—of the order of the magnetocrystalline anisotropy energy (10^5-10^6 erg/cm³). Moreover, in the rather frequently encountered weakly anisotropic magnetic materials, the energy difference of states of strongly differing direction of magnetization is determined by an interaction of a different nature—the magnetoelastic interaction, which amounts to about 10^2 erg/cm³. Let us consider magnetoelastic crystals whose energy is written in the form

$$F_{me} = \hat{B} \hat{u} \hat{M} \hat{M}_S^2.$$

Here \hat{B} is the tensor of the magnetoelastic moduli. This interaction couples the spin and sound waves, so as to realize a situation that is most interesting from the standpoint of nonlinear dynamics, in which excitations of different physical nature and different “levels” of nonlinearity prove to be coupled in the solid.

In any normal mode of coupled oscillations, generally all degrees of freedom of the interacting “partial” (see Ref. 2) subsystems are simultaneously excited. If even one of the subsystems or the coupling between them is nonlinear, the normal modes will also be nonlinear. Under resonance conditions, i.e., when the spectra of the partial subsystems intersect, the energy will be partitioned equally among them. Evidently, here the major contribution to the nonlinearity of the coupled waves must be introduced by the subsystem for which strong nonlinearity is realized at the least energy density of excitation.

Far from resonance each of the normal modes maintains to a considerable degree the physical individuality of the partial subsystem to which it is closest in frequency. Nevertheless the contribution of the interaction of vibrations to the nonlinearity of a concrete mixed mode can prove decisive. An example of such a situation in very simple dynamical systems is the low-frequency mode of the normal vibrations of two coupled pendulums of substantially different

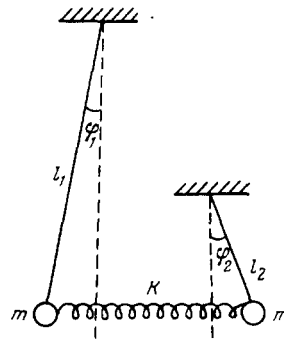


FIG. 1. A very simple example of a dynamic system with strong effective nonlinearity of the low-frequency normal mode ($l_1 \gg l_2$).³

lengths ($l_1 \gg l_2$) (Fig. 1). The amplitudes of the vibrations of the subsystems in the mode under study are coupled by the relationship $\varphi_2 = \xi (\omega_1 l_1 / \omega_2 l_2) \varphi_1$, where $\xi = K / m \omega_1 \omega_2$ is the coupling coefficient ($0 < \xi < 1$), while ω_1 and ω_2 are the “partial” frequencies, i.e., the frequencies of vibration of each of the pendulums when the position of the other is fixed; K is the stiffness of the elastic coupling. With strong enough coupling the condition $\varphi_2 \gg \varphi_1$ can be realized. Consequently the nonlinearity of the low-frequency mode proves substantial even at a relatively low amplitude of excitation of the low-frequency subsystem (if $\varphi_2 \approx 1$ with $\varphi_1 \ll 1$).

To a certain degree analogous features are manifested in the nonlinear properties of the so-called sound-like magnetoelastic waves in magnetics, i.e., waves of the acoustic (gapless) branch of the spectrum of coupled excitations. If the magnetic anisotropy is weak, sonic deformations of relatively small amplitude can give rise to considerable deviations of the magnetic moments from the equilibrium direction. The magnetostrictive elastic stresses, which depend nonlinearly on the amplitude of the spin oscillations, consequently prove to depend nonlinearly also on the amplitude of the deformations in the acoustic wave. The nonlinearity of the dependence of the elastic stresses on the strains amounts to nothing other than elastic anharmonicity, which in this case is introduced into the acoustic vibrations by the interaction of the sound with the spin subsystem of the crystal. This “effective” anharmonicity, which reflects the nonlinearity of the mixed modes, is the fundamental mechanism that determines the intensity of a number of nonlinear wave processes in magnetics.

A fact that appears important in principle from the standpoint of possible generalizations is that the effective anharmonicity substantially alters the characteristic scale discussed above for the amplitude of deformations in the nonlinear acoustic vibrations of a crystal. We can easily estimate this change by using the following qualitative arguments. We can consider a magnetoelastic wave to be weakly nonlinear if both the elastic deformations and the relative amplitudes of the magnetic oscillations ($|\Delta M| / M_S \ll 1$) accompanying the elastic wave are small in it. In the first (“harmonic”) approximation the amplitude ΔM equals the derivative of the effective magnetostrictive field

$$h_{me} = - \frac{\partial F_{me}}{\partial \hat{M}} = - \frac{\hat{B} \hat{u} \hat{M}_S}{M_S^2},$$

caused by the alternating deformation \hat{u} with respect to the

low-frequency dynamic magnetic susceptibility χ . (Henceforth in discussing general problems we do not need to focus attention on the tensor or vector nature of particular quantities. Hence we shall omit the corresponding symbols in formulas, used to obtain estimates bearing in mind that appropriate contractions or essential components of tensors will figure in the concrete relationships.) Weak nonlinearity of a magnetoelastic wave corresponds to the condition $\chi B u_- / M_S^2 \ll 1$. It can be expressed in terms of the coefficients of magnetoelastic (magnon-phonon) coupling $\zeta = (\chi B^2 / C^{(2)} M_S^2)^{1/2}$ by the relationship $\zeta^2 u_- C^{(2)} B^{(-1)} \ll 1$. Finally, noting that the ratio $B / C^{(2)} \approx u_0$ determines the magnitude of the equilibrium ("spontaneous") magnetostrictive deformation, we derive the following quantitative criterion for weak nonlinearity of a magnetoelastic wave of the acoustic branch of the spectrum: $\kappa \equiv \zeta^2 |u_- / u_0| \ll 1$. The quantity κ plays the role of the parameter of the anharmonic expansion of the energy density of the crystal in the dynamic deformations. Usually the magnitude of κ does not exceed $(10-10^2) |u_-|$. In magnetostrictive ferroelectrics having the characteristic parameters $\chi \sim \gamma M_S / \omega_{f_0}$, where ω_{f_0} is the ferromagnetic-resonance frequency, we have $\zeta^2 \approx \gamma B^2 / C^{(2)} M_S \omega_{f_0} \sim 10^{-2}$, $|u_0| \sim 10^5$, and the magnitude of κ is substantially larger: $\kappa \sim 10^3 |u_-|$. However, up to deformations close to the limit for breakdown of real crystals, the nonlinearity proves weak enough and the conditions of applicability of the anharmonic expansions do not break down. We should call attention to the fact that materials with anomalously large magnetostriction, such as the compounds of the rare-earth metals, do not constitute a suitable object of study of nonlinear acoustic phenomena, since in these materials appreciable coupling is attained by increase in $|u_0|$, and this diminishes κ for given values of $|u_-|$.

Employing the above relationships, we can estimate the magnitude of the effective anharmonic moduli arising from the coupling of the elastic and magnetic subsystems. In the linear approximation ("zero-order" in the parameter κ), the magnetoelastic interaction is manifested primarily in the renormalization of the velocity of the acoustic wave. This renormalization can be put into correspondence with the effective values of the elastic moduli:

$$\hat{C}_{\text{eff}}^{(2)} \equiv \hat{C}^{(2)} + \Delta \hat{C}^{(2)}.$$

The quantity

$$\frac{1}{2} \Delta \hat{C}^{(2)} \hat{u}_\sim \hat{u}_\sim = -\frac{1}{2} \zeta^2 C^{(2)} \hat{u}_\sim \hat{u}_\sim$$

amounts to the magnetoelastic (more exactly—the magnetoacoustic) contribution to the potential-energy density. The first anharmonic term of the expansion of the energy density in the deformations, which arises from the magnetoelastic interaction, is of the following order of magnitude in the parameter κ :

$$|\Delta \hat{C}^{(3)} \hat{u}_\sim \hat{u}_\sim \hat{u}_\sim| \sim \kappa |\Delta \hat{C}^{(2)} \hat{u}_\sim \hat{u}_\sim| \sim C^{(2)} \zeta^4 \left| \frac{u_-^3}{u_0} \right|.$$

Taking into account the values presented above of the magnetostrictive constants and the coupling coefficients for ferroelectrics, we obtain the estimate $\Delta C^{(3)} / C^{(2)} \sim 10$, which is close to the ratio $C^{(3)} / C^{(2)}$ in nonmagnetic crystals (we recall

that the coupling coefficient ζ is proportional to the magnitude of $|u_0|$ when $\zeta \ll 1$). Thus, although taking into account the magnetostrictive coupling leads to a relatively slower convergence of the anharmonic expansion, the effective anharmonic moduli of lowest order

$$\hat{C}_{\text{eff}}^{(3)} = \hat{C}^{(3)} + \Delta \hat{C}^{(3)}$$

for ferroelectrics usually differ little from the corresponding moduli of nonmagnetic crystals.

A different situation arises in crystals having strong magnon-phonon coupling, which include, e.g., antiferromagnetics with a magnetic anisotropy of the "easy-plane" type (EPAFs) and a high Neel temperature (T_N), such as hematite ($\alpha\text{-Fe}_2\text{O}_3$, $T_N = 960$ K; see Ref. 4) or iron borate (FeBO_3 , $T_N = 348$ K; see Ref. 5). For certain types of acoustic vibrations the magnitude of the square of the coupling coefficient ζ^2 reaches tens of percent in these materials,^{6,7} although the magnetoelastic interaction in them is quite ordinary (the saturation magnetostriction u_0 is of the order of 10^{-5}).⁸ Here the magnetic contribution to the anharmonic moduli can amount to $\Delta C^3 \sim (10^3-10^4) C^{(2)}$ (see the first estimates made in Ref. 7b). Such a strong anharmonicity, which exceeds the intrinsic anharmonicity of the crystal lattice ($C_{\text{eff}}^{(3)} \approx \Delta C^{(3)} \gg C^{(3)}$) can be called giant without exaggerating.

Crystals of EPAFs are beginning to play an ever more appreciable role in modern nonlinear magnetoacoustics. Hence we shall treat in detail in the next section the features of the nonlinear dynamics of these materials (for their linear dynamics, see Refs. 9-12).

2. NONLINEAR MAGNETOELASTIC DYNAMICS OF ANTIFERROMAGNETICS WITH ANISOTROPY OF THE "EASY-PLANE" TYPE

The magnetoelastic vibrations in an antiferromagnetic in the two-sublattice model are described phenomenologically by a coupled system of nonlinear equations of precession of the vectors of the magnetization of the sublattices \mathbf{M}_1 and \mathbf{M}_2 and the equations of elasticity:

$$-\gamma^{-1} \dot{\mathbf{M}}_n = \{\mathbf{M}_n, \mathbf{H}_n\} \quad (n = 1, 2), \quad (1)$$

$$\rho \dot{U}_i = \frac{\partial \sigma_{ij}}{\partial x_j} \quad (i, j = 1, 2, 3). \quad (2)$$

Here the effective field is

$$\mathbf{H}_n \equiv -\frac{\delta \int F dV}{\delta \mathbf{M}_n},$$

the displacement vector is U_i , and the tensor of the elastic stresses is

$$\sigma_{ij} = \frac{\delta F}{\delta (\partial U_i / \partial x_j)}.$$

The energy density of the crystal is

$$F(\mathbf{M}_1, \mathbf{M}_2, \frac{\partial \mathbf{M}_1}{\partial x_i}, \frac{\partial \mathbf{M}_2}{\partial x_j}, \frac{\partial U_i}{\partial x_j}).$$

In its magnetic component F_m we shall take account of the energy of intersublattice exchange interaction, the Dzyaloshinskii interaction, the uniaxial anisotropy energy (with the effective fields respectively of H_E , H_D , and H_A), and the energy of interaction of the magnetic moments with the external field H :

$$F_m = 2M_0 \left[\frac{1}{2} H_E m^2 - H_D [\mathbf{m}]_z + \frac{1}{2} H_A l_z^2 - (\mathbf{m}\mathbf{H}) - \frac{\alpha}{2} \left(\frac{\partial l_i}{\partial x_j} \right)^2 \right].$$

Here $\mathbf{m} = (\mathbf{M}_1 + \mathbf{M}_2)/2M_0$ is the ferromagnetic vector, $\mathbf{l} \equiv (\mathbf{M}_1 - \mathbf{M}_2)/2M_0$ is the antiferromagnetism vector, $\alpha \equiv v_m^2/4H_E\gamma^2$, and v_m is the so-called "limiting" velocity of the spin waves (magnons), which is proportional to the exchange field and the square of the lattice constant.

The effective exchange field $H_E \sim kT_N/\mu_B$ in crystals having a high enough Neel temperature T_N considerably exceeds the fields of the relativistic (H_A) and exchange-relativistic (H_D) interactions, just as it does the external fields (H) used in experiments. For example, in crystals of α - Fe_2O_3 the characteristic values of the fields are the following: $H_E \approx 10^7$ Oe, $H_D \approx 2 \times 10^4$ Oe, and $H_A \approx 2 \times 10^2$ Oe. In many cases, taking account of the actually existing hierarchy of interactions in the spin system enables one substantially to simplify the description of the nonlinear dynamics of antiferromagnets. In the first approximation in the parameter $\tilde{H}/H_E \ll 1$, where $\tilde{H} = H_D, H_A$, or H , it proves possible to reduce the system of precession equations to the equation of motion for the antiferromagnetism vector \mathbf{l} alone, since $l^2 = 1 - m^2 \approx 1$ and $m \ll 1$ ¹³⁻¹⁵:

$$\begin{aligned} [\dot{\tilde{\mathcal{L}}}] &= 0, \\ \tilde{\mathcal{L}} &= \gamma^{-2} (\dot{\mathbf{l}} - v_m^2 \nabla^2 \mathbf{l}) - \gamma^{-1} \{2[\mathbf{H}\dot{\mathbf{l}}] + [\dot{\mathbf{H}}\mathbf{l}]\} \\ &\quad + \mathbf{H}(\mathbf{H}\mathbf{l}) + H_D[\mathbf{H}\mathbf{z}] + (2H_E H_A + H_D^2) l_z \mathbf{z} - 2H_E \mathbf{H} m_e. \end{aligned} \quad (3)$$

In this approximation it suffices to restrict the treatment in the expression for the magnetoelastic energy density to taking account of invariants of the type

$$F_{ml}^{(l)} = l (\hat{B}_l \dot{u}). \quad (4)$$

Here \hat{B}_l is the tensor of magnetoelastic constants corresponding to the antiferromagnetic vector.

The spin-wave vector of an EPAF, which can be found from the linearized Eq. (3) or, as is usual, directly from the linearized system (1), contains two branches. Their frequencies *without allowance* for the magnetoelastic interaction are given by the relationships

$$\tilde{\omega}_{\mathbf{a}\mathbf{k}}^2 = \gamma^2 [2H_E H_A + H_D (H + H_D)] + v_m^2 k^2, \quad (5)$$

$$\tilde{\omega}_{\mathbf{f}\mathbf{k}}^2 = \gamma^2 H (H + H_D) + v_m^2 k^2. \quad (6)$$

One of the branches (the "antiferromagnetic" one, $\tilde{\omega}_{\mathbf{a}\mathbf{k}}$) has the relatively high activation energy $\gamma(2H_E H_A)^{1/2}$. For example, for α - Fe_2O_3 $\tilde{\omega}_{\mathbf{a}\mathbf{k}}$ lies in the millimeter UHF range.¹⁶ The other "quasiferromagnetic" branch $\tilde{\omega}_{\mathbf{f}\mathbf{k}}$ amounts to the "soft mode" of the spin system, whose activation energy is small, in line with the smallness of the external field intensity. The activation branch of the spectrum $\tilde{\omega}_{\mathbf{a}\mathbf{k}}$ corresponds to vibrations with departure of the vector \mathbf{l} from the base plane and with change of the angle of inclination of the magnetic sublattices. The soft mode $\tilde{\omega}_{\mathbf{f}\mathbf{k}}$ corresponds to rocking of \mathbf{l} in the base plane and precession of the ferromagnetic vector \mathbf{m} about the equilibrium vector \mathbf{m}_s , as in a ferromagnetic. The interaction of the elastic subsystem with the soft spin-wave mode gives rise to very strong coupling. It determines the fundamental features of the mag-

netoacoustic properties of EPAFs. One can show that, under ordinary conditions of not too high frequencies $\tilde{\omega} \ll \omega_{\mathbf{a}\mathbf{k}}$ and weak magnetostrictive fields $H_{me} \ll H_A$, where

$$H_{me} = -\frac{1}{2M_0} \frac{\partial F_{me}}{\partial \mathbf{l}},$$

we can neglect the departure of the antiferromagnetic vector from the base plane in describing the magnetoelastic dynamics ($l_z \approx 0$). Then the equation of motion for \mathbf{l} is reduced to the form

$$\begin{aligned} \gamma^{-2} [\dot{\mathbf{l}} - v_m^2 \nabla^2 \mathbf{l}]_z & \\ = (\mathbf{H}\mathbf{l}) ([\mathbf{H}\mathbf{l}]_z + H_D) + 2H_E [\mathbf{H} m_e]_z + \gamma^{-1} \dot{H}_z. \end{aligned} \quad (7)$$

When we take account of the condition of conservation of the modulus $|\mathbf{l}| = 1$, the only dynamical magnetic variable in Eq. (7) proves to be the angle φ of rotation of the vector \mathbf{l} in the base plane. Transforming to this variable allows us to write the energy density of spin excitations w_m and the magnetoelastic excitation F_{me} in the form

$$w_m = \frac{M_0}{2H_E} [\gamma^{-2} (\dot{\varphi})^2 + \gamma^{-2} v_m^2 (\nabla \varphi)^2 - (H \cos \varphi + H_D)^2], \quad (8)$$

$$F_{me} = (\hat{B}_1(\alpha) \cos 2\varphi + \hat{B}_2(\alpha) \sin 2\varphi) \hat{u}. \quad (9)$$

The explicit form of the components of the tensor of magnetoelastic constants $\hat{B}_n(\alpha)$ ($n = 1, 2$) depends on the concrete symmetry of the crystal and the angle α of orientation of the external field with respect to the unique crystal axis in the base plane. For rhombohedral symmetry, which many of the experimentally studied EPAFs possess (α - Fe_2O_3 , FeBO_3 , MnCO_3 , CoCO_3 , having the space group D_{3d}^6 and the unique axis $x \parallel U_2$), the following relationships hold:

$$\begin{aligned} \hat{B}_1(\alpha) &= \hat{B}_1(0) \cos 2\alpha + \hat{B}_2(0) \sin 2\alpha, \\ \hat{B}_2(\alpha) &= -\hat{B}_1(0) \sin 2\alpha + \hat{B}_2(0) \cos 2\alpha, \\ \hat{B}_1(0) \hat{u} &= -\frac{1}{2} (B_{11} - B_{12}) (u_{xx} - u_{yy}) - 2B_{14} u_{yz}, \\ \hat{B}_2(0) \hat{u} &= -(B_{11} - B_{12}) u_{xy} - 2B_{14} u_{xz}. \end{aligned} \quad (10)$$

Thus it proves possible to describe phenomenologically the magnetoelastic dynamics of EPAFs by using the four-vector magnetoelastic displacement (\mathbf{U}, φ) , which satisfies the system of equations of motion⁵⁰

$$\begin{aligned} \rho \ddot{U}_i &= \frac{\partial}{\partial x_j} (\hat{c}^{(2)} u_{\sim} + \hat{B}_1(\alpha) \cos 2\varphi + \hat{B}_2(\alpha) \sin 2\varphi)_{ij} \\ &\equiv \frac{\partial}{\partial x_j} \sigma_{ij}, \end{aligned} \quad (11)$$

$$\begin{aligned} \gamma^{-2} (v_m^2 \nabla^2 \varphi - \ddot{\varphi}) &= \frac{1}{2} (\gamma^{-2} \omega_{l0}^2 - H H_D) \sin 2\varphi \\ &\quad + H H_D \sin \varphi + \frac{2H_E}{M_0} \\ &\quad \times \{ \hat{B}_2(\alpha) \hat{u} \cos 2\varphi - \hat{B}_1(\alpha) \hat{u}_{\sim} \sin 2\varphi \}, \end{aligned} \quad (12)$$

here $\hat{u}_{\sim} \equiv \hat{u} - \hat{u}_0$, and $\hat{u}_0 = -[\hat{c}^{(2)}]^{-1} \hat{B}_1(\alpha)$ is the tensor of spontaneous magnetostrictive deformations,

$$\omega_{l0} = \gamma [H (H + H_D) + 2H_E H_{ms}^{(s)}]^{1/2}$$

is the frequency of the ferromode of the antiferromagnetic resonance (AFMR), $H_{ms}^{(s)} = -(2/M_0) \hat{B}_1(\alpha) \hat{u}_0$ is the magnitude of the effective spontaneous-striction field; and we have

$$\hat{u} \equiv \frac{1}{2} \left(\frac{\partial U_i}{\partial x_j} + \frac{\partial U_j}{\partial x_i} \right).$$

We should note that using Eqs. (11) and (12) does not presuppose any restrictions on the amplitude of the spin oscillations. They are suitable for describing both weakly and strongly nonlinear effects to which anharmonic approximations are inapplicable. We note also that one can derive Eq. (12) directly from the relationships (8) and (9) by variation methods. It has the form of the well known double sine-Gordon equation⁶⁹ supplemented by nonlinear dynamical couplings. It is encountered in the theory of nonlinear spin excitations in liquid ³He and in the theory of self-induced optical transparency. Antiferromagnetics are another example of physical systems whose description can be reduced to an equation of this type. Here the nonlinear dynamical couplings considerably enrich the pattern of possible wave processes.

3. COUPLED MAGNETOELASTIC WAVES IN ANTIFERROMAGNETICS WITH ANISOTROPY OF THE "EASY-PLANE" TYPE

Let us take up in greater detail the properties of coupled magnetoelastic excitations of small amplitude. Their spectrum Ω_k is determined by the well-known dispersion equation, which can be easily derived from the system (11), (12) linearized over small deviations $\varphi \ll 1$:

$$(\omega_{fk}^2 - \Omega_k^2) - \sum_{S=1}^3 \frac{\zeta_{Sk}^2 \omega_{fk}^2 \omega_{Sk}^2}{\Omega_k^2 - \omega_{Sk}^2} = 0. \quad (13)$$

Here ω_{Sk} is the partial frequency of the concrete ($S = 1, 2, 3$) elastic mode having the wave vector \mathbf{k} and the polarization $\mathbf{e}^{(S)}$, and ω_{fk} is the partial frequency of the ferromode. The adjective "partial" is essential—it means that the frequencies ω_{Sk} and ω_{fk} that enter into (13) are calculated for a fixed partner subsystem (see the text above accompanying Fig. 1). For example, ω_{fk} is calculated for a "frozen" lattice (for more details on this, see Ref. 12). Therefore it contains the so-called magnetoelastic gap: $\omega_{fk} = (\omega_{fk}^{(0)2} + 2\gamma^2 H_E H_{mS}^{(0)})^{1/2}$. The magnon-phonon coupling coefficient ζ_{Sk} is determined by the relationship

$$\zeta_{Sk}^2 = \frac{H_E}{M_0} \frac{(2\hat{B}_2 u_S)^2}{(\omega_{fk}/\gamma)^2 \hat{C}^{(2)} u_S \hat{u}_S}, \quad (14)$$

$$(\hat{u}_S)_{ij} = \frac{1}{2k} (e_i^{(S)} k_j + e_j^{(S)} k_i).$$

The asymptotic linearity in k (i.e., when $k \gg k_m \equiv \omega_{f0}/v_m$, Fig. 2) of the spin-wave spectrum in an antiferromagnet determines the qualitative differences of the spectra of magnetoelastic excitations in crystals having a high and a low Neel temperature T_N , to which the "limiting" magnon velocity v_m is related by direct proportionality. In low temperatures EPAFs (such as MnCO_3 , CoCO_3 , and CsMnF_3), T_N is lower than the Debye temperature T_D and the velocity of spin waves is smaller than the velocity of sound (see Fig. 2b). Here the spectra of the "pure" (partial) spin and elastic excitations ω_{fk} and ω_{Sk} intersect. The conditions for strongest interaction are realized in the resonance region near the intersection. In high-temperature EPAFs ($T_N > T_D$), for which $v_m > v_S$, intersection of the "partial" spectra is not realized. In this case the spin waves for any k are unambigu-

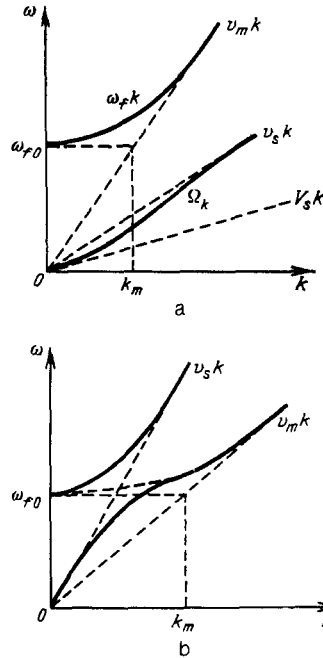


FIG. 2. Spectra of coupled magnetoelastic waves in crystals of an EPAF (solid lines)—high-temperature ($T_N > T_D$) (a) and low-temperature ($T_N < T_D$) (b).^{7c}

ously separated into acoustic (more exactly—soundlike) and spin (magnonlike) waves, while the strongest coupling corresponds to the long-wavelength region of the spectrum ($k \ll \omega_{f0}/v_m$). We note for the discussion below that, in an EPAF of the type of $\alpha\text{-Fe}_2\text{O}_3$ or FeBO_3 , the relation holds that $v_S^2 \ll v_m^2$, and the frequencies of the acoustic waves satisfy the condition $\Omega_k^2 \ll \omega_{fk}^2$ for any wave vectors \mathbf{k} .

Magnetoelastic coupling renormalizes the velocities of the acoustic waves and causes them to depend on the field intensity. The acoustic waves contain a substantial admixture of "nonresonance" spin excitations caused by the deformations. Their amplitude can be found from the linearized equation (11) with allowance for the condition $\partial/\partial t \ll \omega_{fk}$:

$$q_{\mathbf{k}} = -\frac{2H_E}{M_0} \left(\frac{\gamma}{\omega_{fk}} \right)^2 \hat{B}_2 \hat{u}_{\mathbf{k}}. \quad (15)$$

It is precisely these excitations, participating in nonlinear interactions inherent in the spin system, that introduce anharmonicity into the acoustic vibrations. We can easily convince ourselves that in weak magnetic fields, and namely when $H(H + H_D) \lesssim 2H_E H_{mS}$, the amplitudes of the nonresonance excitations prove to be large ($\varphi \sim 1$) even at deformations of the order of the spontaneous deformations ($u_{\mathbf{k}} \sim u_0$). The nonlinearity of the acoustic modes under these conditions *cannot be considered to be weak*.

When $u_{\mathbf{k}} \ll u_0$ and $\varphi \ll 1$ the elastic-stress tensor can be linearized and reduced to the usual form $\hat{\sigma}_{\mathbf{k}} = C_{\text{eff}}^{(2)}(\mathbf{k}) \hat{u}_{\mathbf{k}}$, where the effective second-order elastic moduli, i.e., those renormalized by the interaction, are determined by the relationships¹¹

$$\hat{C}_{\text{eff}}^{(2)}(\mathbf{k}) \equiv \hat{C}^{(2)} + \Delta \hat{C}^{(2)}(\mathbf{k}), \quad (16)$$

$$\Delta \hat{C}^{(2)}(\mathbf{k}) = -\frac{H_E}{M_0} \left(\frac{2\gamma \hat{B}_2}{\omega_{fk}} \right)^2. \quad (17)$$

The spectrum and polarization of the magnetoelastic waves of the acoustic branch are found here, as in ordinary elasticity theory, from an equation like the Green-Christoffel equation:

$$[\rho\Omega_k^2 \hat{\Gamma} - \hat{\Gamma}_{\text{eff}}(\mathbf{k})] \epsilon_{\mathbf{k}} = 0, \quad (18)$$

where we have

$$\hat{\Gamma}_{\text{eff}} = \hat{C}_{\text{eff}}^{(2)} \mathbf{k} \mathbf{k}.$$

The field dependence of the moduli $\hat{C}_{\text{eff}}^{(2)}(H)$ and of the corresponding velocities of sound bear direct information on the magnitude of the linear coupling of the elastic and spin waves. In the simplest case of interaction of one elastic mode (S) with the spin system, the field dependence of the velocity of sound is described by the relationship

$$V_{S\mathbf{k}}(H) = v_{S\mathbf{k}}(1 - \xi_{S\mathbf{k}}^2(H))^{1/2}. \quad (19)$$

The specific participation of the exchange reaction, which is characteristic specifically of antiferromagnetics,¹⁷ in the formation of the amplitudes of the interaction of the excitations⁹ and the magnetoelastic activation of the spectrum of spin waves¹⁰ has the result that the coupling coefficient proves to be of the order of unity over a broad interval of magnetic fields $0 < H(H + H_D) \leq 2H_E H_{\text{ms}}^{(0)}$ that considerably exceeds the monodomianization field of the crystal. For hematite the characteristic field is $H^* = 2H_E H_{\text{ms}}^{(0)} / H_D \approx 0.5$ kOe.

The acoustic modes that satisfy the condition of limiting strong coupling $\xi_{S,\mathbf{k} \rightarrow 0}(H \rightarrow 0) \rightarrow 1$ are of fundamental physical and practical interest. The existence of such modes in a crystal that is isotropic in its magnetic properties (though not necessarily in its magnetoelastic properties) involves losses of stability of the equilibrium state with respect to slow rotation of the magnetization in the xy plane by an arbitrary angle (with a corresponding change in the spontaneous deformation). In many ways the situation is analogous to an orientational phase transition^{7c,18} and allows interesting analogies with systems having spontaneously broken symmetry.¹²

Measurement of the field dependence of the velocity of sound is one of the fundamental methods of experimental study of the coupling of acoustic with spin waves. Figure 3 shows the data of measurements of the velocities of certain types of running bulk and surface acoustic waves in hematite^{21,20}. Also shown there are the results of measurement of the intrinsic frequency of acoustic vibrations of the "contour-shear" mode for a resonator made of $\alpha\text{-Fe}_2\text{O}_3$ in the form of a disk cut in the base plane.²¹ The results of calculations performed by the methods of elasticity theory using the effective moduli $\hat{C}_{\text{eff}}^{(2)}(k \rightarrow 0, H)$ are presented at the same time. The differing symmetries of the tensors $\hat{C}^{(2)}$ and $\hat{C}_{\text{eff}}^{(2)}$ lead to removal of the degeneracy of the spectrum of transverse waves propagating along the trigonal axis of rhombohedral EPAFs. One of the normal modes is characterized by strong coupling, whereas the other one does not interact linearly with the spin system (see the curves l' and l'' in Fig. 3).

The interest in the properties of the contour-shear mode arises from the fact that, according to the calculations,²¹ specifically it satisfies the criterion of limiting strong coupling. The field dependence of its frequency is described by a relationship analogous to that derived in Refs. 13 and 18 for

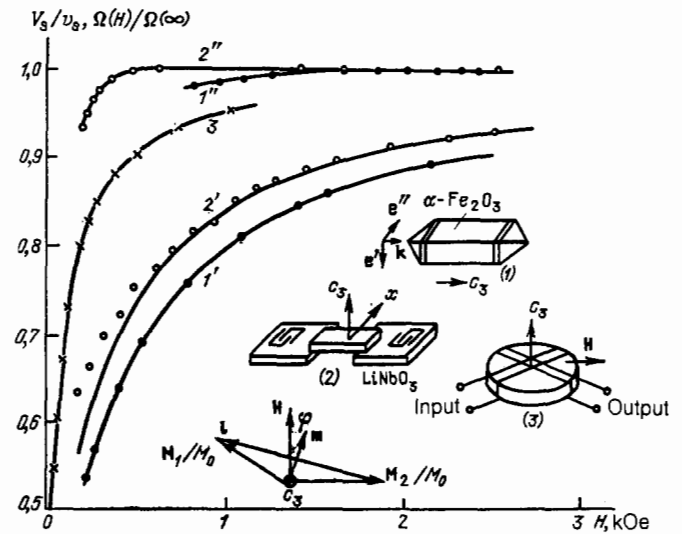


FIG. 3. Dependence of the normalized velocities (curves 1 and 2) and acoustic-resonance frequencies (curve 3) on the magnetic field intensity in $\alpha\text{-Fe}_2\text{O}_3$, l —volume transverse waves ($l - e' \parallel \mathbf{x} \parallel \mathbf{H}$,²⁰ $l - e'' \parallel \mathbf{x} \parallel \mathbf{H}$ ¹⁹); 2 —surface waves ($2' - \mathbf{H}\mathbf{x} = \pi/4$, $2'' - \mathbf{H}\parallel\mathbf{x}$)²¹; 3 —resonance of the shear mode over the contour of the thin disk. Dots—experiment,²¹ lines—calculation. Insets—geometry of excitation and reception of magnetoelastic waves.

running waves:

$$\Omega(H) = \Omega(\infty) \left(1 - \frac{2H_E H_{\text{ms}}'}{\omega_{T0}^2 \gamma^2} \right)^{1/2}.$$

Here the frequency

$$\omega_{T0} = \gamma [H(H + H_D) + 2H_E H_{\text{ms}}']^{1/2}$$

differs from the experimentally measured antiferromagnetic resonance frequency by the amount of the magnetoelastic gap. The data presented in Fig. 3 imply that the magnetoelastic interaction leads to a variation in the frequencies and velocities of the bulk acoustic waves by a factor of practically two (i.e., fourfold for the corresponding dynamical moduli), while the variation in the velocities of surface acoustic waves reaches 35%. Such a substantial renormalization of the acoustic parameters is direct experimental proof of the strong coupling of the elastic and spin waves in $\alpha\text{-Fe}_2\text{O}_3$ crystals. Magnetoelastic waves in FeBO_3 possess analogous properties.⁶ Similar strongly coupled modes are the fundamental objects of experimental studies in the nonlinear magnetoacoustics of high-temperature EPAFs.

The gist of this section, which would be difficult to believe without the presented proofs, is: a quite small change in the magnetic field, e.g., from 0.03 to 2 kOe, can alter the dynamical stiffness of an antiferromagnetic by a factor of four.

4. EFFECTIVE ANHARMONIC ELASTIC MODULI OF ANTIFERROMAGNETICS WITH ANISOTROPY OF THE "EASY PLANE" TYPE

In the lowest order of perturbation theory, anharmonicity of excitations of the acoustic branch of the spectrum arises from the nonlinearity of the magnetoelastic interaction, as well as from pure elastic nonlinearity.¹³ The expansion of the magnetoelastic energy density of (9) in a power

series in the amplitudes φ of the spin oscillations contains the anharmonic term

$$F_{me}^{(3)} = -2\hat{B}_1\hat{u}\varphi^2. \quad (20)$$

Equation (20) describes processes of interaction of one sound wave and two spin waves. Upon taking account of the spin oscillations of (15) that accompany the sound wave, we can easily isolate the contribution to the energy density of the acoustic excitation, which is proportional to the cube of the deformation. One can correlate this contribution with the tensor of the anharmonic elastic moduli $\Delta\hat{C}^{(3)}$ ¹³:

$$\Delta w^{(3)} = \frac{1}{3!} \Delta\hat{C}^{(3)}\hat{u}\hat{u}\hat{u}, \quad (21)$$

$$\Delta\hat{C}^{(3)} = -6 \left(\frac{H_E}{M_0} \right)^2 \frac{(2\hat{B}_1)(2\hat{B}_2)^2}{(\omega_{t0}/\gamma)^4}.$$

For simplicity we have restricted the treatment to the long-wavelength region of the spectrum, i.e., $\omega \ll \omega_{t0} \approx \omega_{nk}$. Using the characteristic parameters $B \sim 10^7$ erg/cm³, $H_E/M_0 \sim 10^4$, and $(\omega_{t0}/\gamma)^2 \sim 10^7$ erg/cm³, we obtain for α -Fe₂O₃ at $H \sim 1$ kOe the estimate presented above of $\Delta C^{(3)} \sim 10^4 C^{(2)} \sim 10^{16}$ erg/cm³.

Equation (21) describes processes of interaction of three acoustic (soundlike) waves. A number of experimentally observable nonlinear acoustic phenomena require account to be taken of a higher-order effective nonlinearity to describe them. The magnetic and magnetoelastic energies of the crystal contain anharmonic terms of all orders in the amplitudes of the magnetoelastic excitations. The effective fourth-order elastic moduli are formed by three fundamental mechanisms: four-wave interaction of non-resonance-excited spin waves, magnetoelastic interaction with participation of a sound wave and three nonresonance spin waves, and the interaction of (20) in second-order perturbation theory.^{24,25} The first two mechanisms correspond to the following terms in the energy density:

$$w^{(4)} = -\frac{M_0}{2H_E} \left[\frac{1}{3} \left(\frac{\omega_{t0}}{\gamma} \right)^2 - \frac{1}{4} HH_D \right] \varphi^4 - \frac{4}{3} \hat{B}_2 \hat{u} \varphi^3. \quad (22)$$

Taking into account all the contributions cited above, the anharmonic terms of the expansion of the energy density of interest to us are reduced to the standard form²⁵:

$$\Delta w^{(4)} = \frac{1}{4!} \Delta\hat{C}^{(4)}\hat{u}\hat{u}\hat{u}\hat{u}.$$

Here we have

$$\Delta\hat{C}^{(4)} = 12 \left(\frac{H_E}{M_0} \right)^3 \frac{(2\hat{B}_2)^4}{(\omega_{t0}/\gamma)^8} \left(1 + \frac{1}{4} \frac{\gamma^2 HH_D}{\omega_{t0}^2} \right) - 48 \left(\frac{H_E}{M_0} \right)^3 \frac{(2\hat{B}_2)^3 (2\hat{B}_1)^2}{(\omega_{t0}/\gamma)^8}. \quad (23)$$

Concerning the symbols $(\hat{B})^n$, see footnote 1). We can easily note that the expansion of the energy density of the acoustic excitations in a power series in the deformations has the structure discussed above of a power series in the parameter $\kappa = \zeta^2 |u/u_0|$. For α -Fe₂O₃ with $H \approx 0.5$ kOe we have $\kappa \approx 10^4 |u_-|$ and $\Delta C^{(4)} \sim 10^{20}$ erg/cm³.

The anomalously large magnitude, specific symmetry, and strong dependence of the effective elastic moduli on the magnitude and direction of the magnetic field facilitate the experimental detection and identification of the magnetoelastic mechanisms of many nonlinear acoustic processes.

5. EXPERIMENTAL NONLINEAR MAGNETOACOUSTICS OF HEMATITE

In the past decade single crystals of α -Fe₂O₃ have become the principal object of intensive study of nonlinear acoustic phenomena in magnetically ordered materials. Strong coupling of the elastic and magnetic subsystems is realized in hematite at room temperature in weak magnetic fields ($H \lesssim 1$ kOe) and in a frequency interval overlapping practically all the ultrasound region. Modern technology allows one to obtain large, high-quality single crystals of hematite.⁶⁴ To a considerable extent all this has facilitated the development of experimental magnetoacoustics.

Direct experimental measurements²⁶ of the effective third-order anharmonic moduli have been performed on synthetic single crystals of α -Fe₂O₃ of dimensions 5×4 mm² in the base plane and 13 mm in length along the C_3 axis. The quality of the crystal was sufficiently high: for the soundlike wave being studied having $k \approx 600$ cm⁻¹, the quality factor was $Q_k = \omega_k / \Delta\omega_k = k / \alpha_k \sim 3 \times 10^3$ for a "turned-off" field $H = 3$ kOe of magnetoelastic coupling (α_k is the decay coefficient for the power of the wave). The nonlinear moduli were determined from the change in the velocities of the acoustic waves under a relatively weak static deformation of the crystal. We note that the anomalously high tensosensitivity of the velocities of sound in EPAFs had been predicted also in Ref. 7b—on the basis of analysis of the doubly linear effects of static elastic stresses on the antiferromagnetic resonance frequency and the magnetoelastic coupling. In Ref. 26 the geometry of experiment was chosen taking into account the strong magnetoelastic anisotropy of hematite, owing to which the anharmonic moduli ΔC_{455} and ΔC_{155} have the largest magnitude³ (with \mathbf{H} parallel to the twofold axis $U_2 \parallel \mathbf{x}$). In determining these components of the tensor $\Delta C^{(3)}$, one can use a transverse wave with polarization $\mathbf{e} \parallel \mathbf{x}$ and wave vector $\mathbf{k} \parallel \mathbf{z}$. Here one must create static stresses of two types that are homogeneous throughout the crystal: tensile (σ_{yy}) and shear (σ_{yz}). An acoustic wave at the frequency 30 MHz was excited and detected with piezotransducers. The variation of the velocity of this transverse wave δv_i upon deforming the crystal was measured from the change in the phase of the signal in the receiving transducer. The results were processed by using the relationships

$$\Delta C_{155} = \frac{1}{2} [C_{44}(c_{11} - c_{12}) S_{\parallel}(H) + C_{44} C_{44} S_{\perp}(H)], \quad (24)$$

$$\Delta C_{455} = \frac{1}{2} [C_{44}^2 S_{\perp}(H) + 2C_{44} C_{44} S_{\parallel}(H)].$$

Here we have

$$S_{\parallel} \equiv -\frac{\rho (\delta v_i^2)_{\parallel}}{C_{44} \sigma_{yy}},$$

$$S_{\perp} \equiv \frac{\rho (\delta v_i^2)_{\perp}}{C_{44} \sigma_{yz}}.$$

The subscripts \parallel and \perp correspond to tensile and shear deformations. The results of the measurements and of calculation of the modulus $\Delta C_{455}(H)$ ²⁶ are presented in Fig. 4.

The use of static deformation for determining the dynamical fourth-order elastic moduli (e.g., from its influence on frequency doubling of sound) involves a fundamental difficulty. The static deformations that cause the change in the velocity of the magnetoelastic wave owing to fourth-order anharmonicity alter the direction of the equilibrium magne-

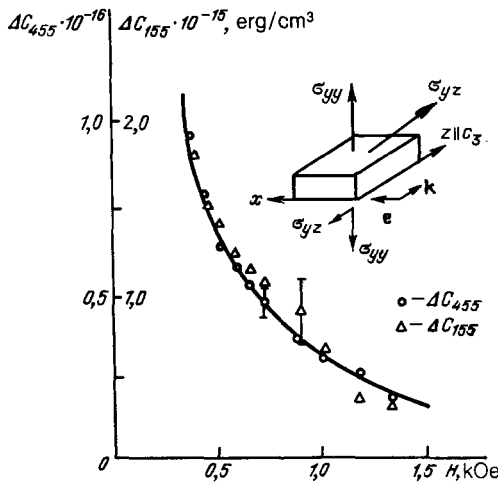


FIG. 4. Dependences of the effective third-order elastic moduli on the magnetic field intensity (solid line—calculation by Eqs. (21)).²⁶

tization. Since the magnetostrictive field that determines the gap in the spectrum of spin waves does not hinder static remagnetization, in contrast to high-frequency remagnetization, the deviation of the magnetic moments (and the changes in the velocity of sound associated with them) in static and dynamic deformation can differ substantially. Accordingly the need arises of distinguishing the dynamic and quasistatic moduli. As $H \rightarrow 0$ and near orientational phase transitions, the latter diverge proportionally to $1/(\omega_0^2 - 2\gamma^2 H_E H_{ms})^n$, where n is the order of the expansion of the energy density in the components of the static-deformation tensor that are associated with the change in the direction of the vector \mathbf{l} in the linear approximation.²⁵

Measurements of the field dependence of the dynamic moduli ΔC_{5555} and ΔC_{6666} have been performed while using the effect of nonlinear frequency shift (NFS) of the magnetoelastic oscillations of a thin plate.^{24,25} In the experiment the acoustic vibrations of a monocrystalline resonator in the form of a disk 0.35-mm thick and 5.5 mm in diameter cut in the base plane were studied. The NFS was measured from the distortion of the shape of the resonance line upon increasing the amplitude of the vibrations (a recording of a characteristic shape of an acoustic resonance line is shown in Fig. 5a). The magnitude of the NFS of the acoustic vibrations is proportional to the fourth-order elastic moduli: ΔC_{5555} for the depth shear mode and ΔC_{6666} for the contour shear mode. Figure 5b compares the results of measurements and calculation of the field dependence of the parameters $\Delta C^{(4)}(H)$. The calculations were performed by using

the relationships

$$\Delta C_{5555} = 12 \left(\frac{H_E}{M_0} \right)^3 \frac{(2B_{14})^4}{(\omega_{f0}^2 \gamma)^8} \left(1 + \frac{\gamma^2 H H_D}{4\omega_{f0}^2} \right),$$

$$\Delta C_{6666} = \frac{3}{2} \frac{[(c_{11} - c_{12})c_{44} - 2c_{14}^2]^2}{M_0 H_{ms}^2 c_{44}^2} \left(\frac{2H_E H_{ms} \gamma^2}{\omega_{f0}^2} \right)^3 \times \left(1 + \frac{\gamma^2 H H_D}{4\omega_{f0}^2} \right). \quad (25)$$

In agreement with the theoretical ideas on the features of the effective elastic anharmonicity, the experiment performed on hematite demonstrates the anomalously large magnitude and strong field dependence of the anharmonic elastic moduli of EPAFs.

One of the first confirmations of the concept of effective elastic anharmonicity was the strong field dependence discovered in $\alpha\text{-Fe}_2\text{O}_3$ of the amplitude of the second acoustic harmonic generated by a running elastic wave.²⁷ A wave at the frequency of 37 MHz was excited at one end of the specimen. At the opposite end the acoustic signal was received with a resonance piezotransducer tuned to the doubled frequency. Figure 6 shows the results of measuring the dependence of the power of the second-harmonic signal on the power of the pump wave and the field dependence of the efficiency of conversion, which is proportional to $\omega_0^{-8}(H)$, in agreement with the theory.¹³ The decline in the efficiency of conversion with decreasing field in weak fields is explained by the increase in damping of the acoustic waves as the homogeneity of the magnetization distribution over the volume of the specimen breaks down—primarily owing to crystal-structure defects, since the disorientation of the magnetization near a defect increases with decreasing field.

At the same time an effect was discovered in hematite of acoustic detection by running waves.^{13,27} The essence of the effect consists in generation of a sound wave at the frequency of the envelope of the amplitude-modulated acoustic signal. The field dependence of the power of the detected signal that was found was also proportional to $\omega_0^{-8}(H)$. Generation of the second acoustic harmonic of a surface magnetoelastic wave was found later²⁸—also for $\alpha\text{-Fe}_2\text{O}_3$.

A convincing demonstration of the strong acoustic nonlinearity of hematite was the observation of the effect predicted in Ref. 13 of stimulated combination scattering (SCS) of running acoustic waves.²⁹ Upon propagation of a "pure" transverse pump wave of frequency ω_p and wave vector \mathbf{k} parallel to the trigonal axis, a threshold process was observed of generation of backward-running magnetoelastic waves at the combination frequencies ω_1 and ω_2 , namely such that $\omega_1 + \omega_2 = \omega_p$.

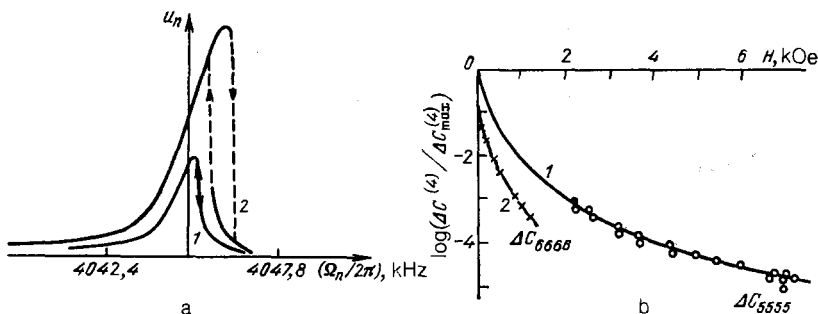


FIG. 5. Nonlinear frequency shift and hysteresis of the amplitude-frequency characteristics of acoustic resonance of the thickness-shear mode observed for different values of the amplitude of the alternating ac field ($h_2/h_1 = 2$, $H = 2$ kOe).²⁴ b—Field dependences of the effective fourth-order elastic moduli (curves—calculation by Eqs. (24), (25)).²⁴

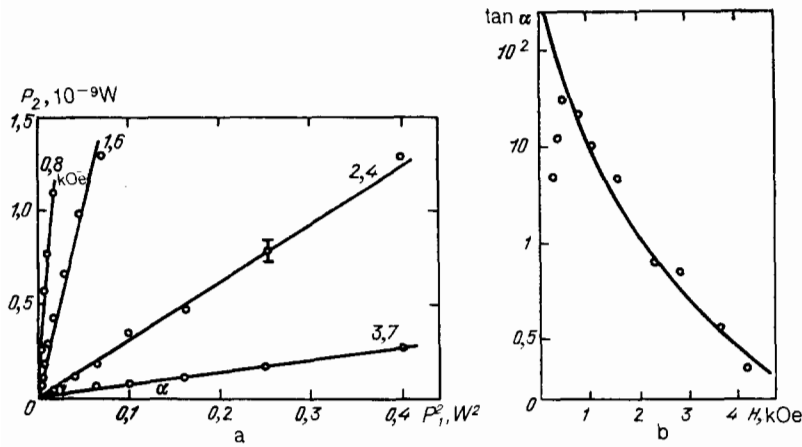


FIG. 6. a—Dependence of the power of the second acoustic harmonic on the square of the power of the pump wave in α -Fe₂O₃.²⁷ b—Field dependence of the efficiency of conversion of sound into the second harmonic (line—calculation).²⁷

The conditions for space-time synchronization for this process are illustrated in Fig. 7a. Since the velocities of magnetoelastic waves (with polarization $\mathbf{e}_{1,2} \parallel \mathbf{H} \parallel \mathbf{x}$) substantially depend on the field intensity (see Fig. 3), the combination frequencies corresponding to the synchronization condition also depend on the field. Figure 7b shows the data of the measurements and the results of calculation of the field dependences of the generation frequencies. Calculation¹³ of the magnitude of the threshold deformation within the framework of the theory of effective anharmonicity for the process being discussed yields the following relationship:

$$u_p^c = \pi \frac{2|B_{14}|}{C_{44}} \frac{(1-\zeta^2)^{3/2}}{k_p L \zeta^5}, \quad (26)$$

$$\zeta^2 = \frac{H_E}{M_0} \frac{(2B_{14}\gamma)^2}{\omega_{f0}^2 C_{44}}.$$

Here L is the length of the specimen.

A calculated estimate of the threshold deformation (u_p^c) $\approx (3.5 \pm 1.5) \times 10^{-7}$ for $H \approx 0.5$ kOe agrees in order of magnitude with the result of measurement of (u_p^c) $\approx (8 \pm 4) \times 10^{-7}$. In the same geometry and also for α -Fe₂O₃ under synchronization conditions, a threshold-free process was observed of merger of magnetoelastic waves into a running pure-sound wave that was the reverse of the SCS.³⁰

Hematite and other antiferromagnetics with giant

acoustic nonlinearity are unique objects for observing acoustic analogs of nonlinear optical phenomena—including those discussed, e.g., in the review of Ref. 31.

When a high-frequency magnetic field $h(t)$ homogeneous throughout the specimen acts on a crystal of α -Fe₂O₃, a number of parametric acoustic phenomena can occur.³² The parametric coupling of sound with an alternating field, just like the effective interactions of elastic waves, is mediated by the excitation of the spins. In an alternating field parallel to the magnetizing field (the so-called parallel pumping ($h_{\parallel} \ll H$)), the following term in the energy density is responsible for the parametric coupling:

$$w_{p\parallel} = \frac{M_0}{2H_E} (2H + H_D) h_{\parallel} \varphi^2. \quad (27)$$

Upon substituting into this the amplitudes of the nonresonance spin oscillations of (15), we obtain the following expression for the coupling of the acoustic waves with the field:

$$w_{p\parallel} = \left(\frac{2H_E}{M_0} \right) \frac{2H + H_D}{(\omega_{f0}/\gamma)^4} (\hat{B}_2 \hat{u})^2 h_{\parallel}. \quad (28)$$

The magnetoelastic interaction of (20) also determines the coupling of the sound with the transverse pump field $h_{\perp}(t)$. Taking into account the nonresonance excitations of the spin system caused by the transverse field ($\varphi_{\perp} = (H + H_D)/$

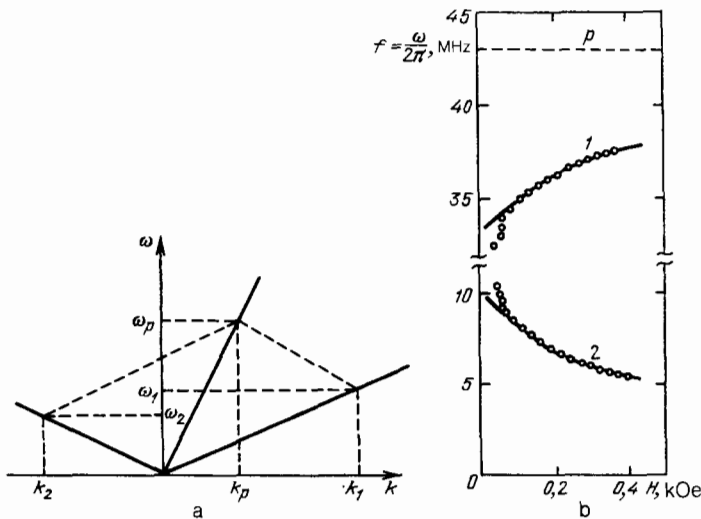


FIG. 7. a—Diagram of the conditions of synchronization for acoustic stimulated combination scattering.¹³ b—Field dependence of the combination frequencies of transverse magnetoelastic waves in α -Fe₂O₃ (p — ω_p , 1— ω_1 , 2— ω_2 , lines—calculation).²⁹

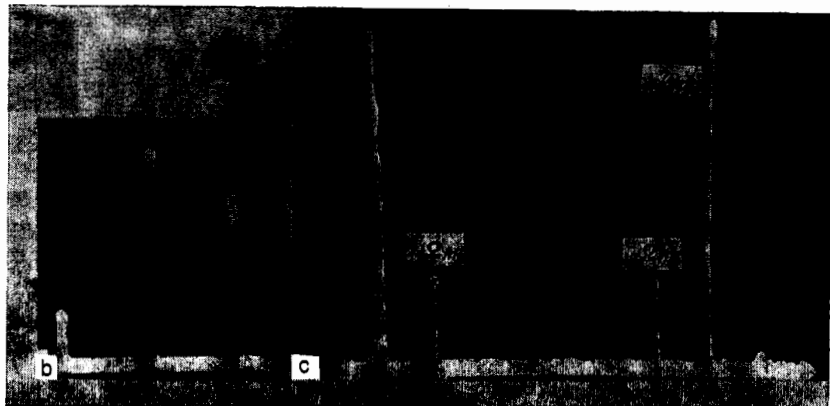
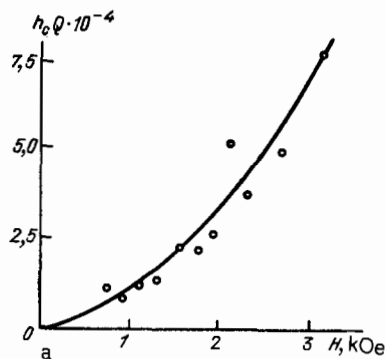


FIG. 8. a—Dependence of the amplitude of the reduced threshold field on the constant magnetic bias field; the reduction point is $H = 1.6$ kOe.³² b—Spectrogram of parametric generation ($\omega_p = 2\Omega_n$).³² c—Spectrogram of parametric generation of magnetoelastic vibrations in a nondegenerate regime ($\omega_p = \Omega_n + \Omega_m$).³²

$(\omega_0/\gamma)^{-2} \perp$ and by the sound (15), we find

$$w_{p\perp} = 8 \frac{H_E}{M_0} \frac{(H+H_D)}{(\omega_{r0}/\gamma)^4} (\hat{B}_1 \hat{u}) (\hat{B}_2 \hat{u}) h_{\perp}. \quad (29)$$

The parametric interactions (28) and (29) allow a graphic physical interpretation. The effective elastic moduli $\Delta C^{(2)}(H)$ (and this implies also the frequencies of the acoustic spectrum and velocities of sound) depend on the magnitude and direction of the external magnetic field. Modulation of the external field in magnitude or in direction leads to modulation of the elastic parameters of the crystal and parametric couplings with the energy $w_p = w_{p\parallel} + w_{p\perp}$, where

$$w_p = - \left(\frac{\partial \Delta C^{(2)}}{\partial H} \right) \mathbf{h} \frac{\hat{u} \hat{u}}{2}. \quad (30)$$

When the amplitude of the ac field with the frequency ω exceeds a critical value, e.g., $h_{\parallel} > h_c = Q^{-1} \Omega / (\partial \Omega / \partial H)$ (Q is the Q -factor of the acoustic mode), a parametric instability arises in α -Fe₂O₃ crystals of the magnetoelastic acoustic modes with the frequency $\Omega = \omega/2$. An analogous effect has been observed earlier in the ferrite garnet Eu₃Fe₅O₁₂.³³ Under the conditions of the experiment the amplitude of the parametric interactions characterized by the quantity $\partial \Delta C^{(2)} / \partial H$ is substantially larger for α -Fe₂O₃ than for the ferrite. Moreover, in hematite the effect is observed over a considerably broader range of magnetic fields.

Figure 8a shows a spectrogram of parametric generation and the field dependence of the threshold field for the acoustic depth-shear mode of a disc acoustic resonator made of α -Fe₂O₃ (the plane of the disk is parallel to the base plane). The pumping and recording of the instability were performed by an induction method. The line in Fig. 8a shows the result of calculation of dependence of h_c from the

data of independent measurements of $Q(H)$ and $\Omega(H) = \Omega(\infty)(1 - \zeta^2(H))^{1/2}$ of the studied specimen. For the characteristic values $Q \approx 10^4$, $H \approx 0.5$ kOe, and $\Omega^{-1} / (\partial \Omega / \partial H) \approx 0.2$ kOe⁻¹, the threshold field has the magnitude $h_c \approx 0.5$ Oe.

When the resonance conditions are satisfied and with an intense enough external agent (pump), one observes the so-called nondegenerate threshold processes of parametric generation of magnetoelastic modes—at the combination frequencies $\Omega_n + \Omega_m = \omega_p$ (see the spectrogram, Fig. 8b).³²

Past the threshold of parametric excitation, the effects of nonlinear self-action of acoustic modes manifest themselves. In particular they are found from the difference of the values of the frequency detuning ($\Delta\omega \equiv -\omega_p - 2\Omega_n$) with respect to the parametric resonance at which sound generation arises and disappears. A characteristic recording of the hysteresis dependence of the amplitude of a parametrically

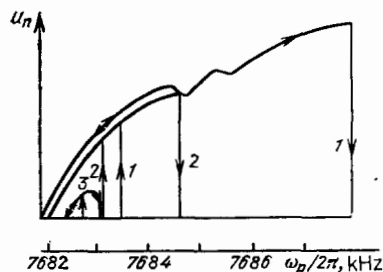


FIG. 9. Dependence of the amplitude of parametric magnetoelastic vibrations on the pump frequency for different degrees of supercriticality h/h_c .³² $h/h_c = 1.63$ (1), 1.27 (2), and 1.02 (3).

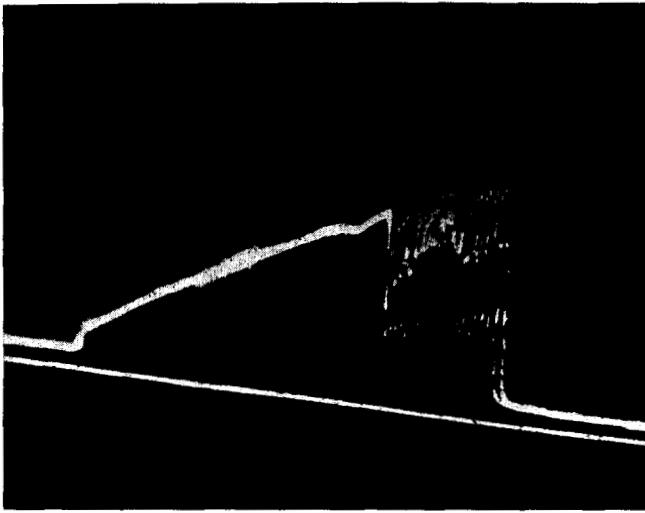


FIG. 10. Characteristic dependence of the amplitude of parametric generation of magnetoelastic vibrations on the pump frequency under conditions of automodulation.²⁵

excited oscillation on the detuning is shown in Fig. 9. A manifestation of self-action and nonlinear intermode interactions proves to be the automodulation of the over-threshold amplitude of deformations observed in $\alpha\text{-Fe}_2\text{O}_3$ ³² in the parametric generation of sound (Fig. 10). The effect arises at values of the magnetic field, supercriticality, and frequency detuning defined for the given mode.

The parametric effects in running acoustic waves also include the frequency shift discovered in hematite of a wave in a non-steady-state, monotonically varying magnetic field.¹⁹

Recently phenomena were observed in $\alpha\text{-Fe}_2\text{O}_3$ of parametric amplification and front reversal of running magnetoelastic waves in a high-frequency magnetic field³⁴—this is also one of the examples of realization of optic-acoustic analogies in the spirit of the concepts summarized in Ref. 31.

The experimentally observable phenomena of generation of long-wavelength nonresonance excitations of the spin system in a field of nonlinearly interacting acoustic waves are associated with the interactions of (28), (29), and (30).³⁵ The acoustic waves give rise in the crystal to oscillations of the magnetization $\mu(t)$ that depend nonlinearly on the elastic deformations. The quadratic components of the ac magnetization can be calculated by using (30): $\mu^{(2)} = -\partial w_p / \partial h$. When harmonic sound waves with wave vectors identical in magnitude propagate in opposite direc-

tions ($k_2 = -k_1$), spatially homogeneous oscillations of the magnetization are excited in the crystal at the sum frequency. In the case of amplitude-modulated waves, the time envelope of the integral of the magnetization over the length L of the interaction region amounts to the convolution function of the envelopes of the interacting waves:

$$\mu(t) \sim \int u_1(\xi) u_2(\xi - 2vt) d\xi.$$

(We assume that L is larger than the spatial extent of the acoustic pulses.) The effect of acoustic convolution was observed in a crystal of $\alpha\text{-Fe}_2\text{O}_3$ ³⁵ upon interaction of transverse bulk waves propagating along the trigonal axis. Sound waves of frequencies $\omega \sim 30$ MHz were excited at opposite ends of the crystal by piezotransducers made of LiNbO_3 . The spatially integrating detection of the signal of magnetization oscillations was performed by an induction method. Figure 11⁷⁰ shows characteristic oscillograms of the convolution signals from one pair (a) and from two pairs (b) of acoustic pulses. In agreement with the theoretical concepts of mediated interactions of the type of (28) and (29), intramode interactions of coupled waves ($\mathbf{e}_1 \parallel \mathbf{x} \parallel \mathbf{H}$) were observed in the experiment with excitation of a longitudinal component of the magnetization $\mu_{\parallel} \sim u_{xz}^2$ and intermode interactions of the coupled and the pure sound waves ($\mathbf{e}_1 \parallel \mathbf{x} \parallel \mathbf{H}$; $\mathbf{e}_2 \perp \mathbf{e}_1$) with excitation of a transverse component $\mu_{\perp} \sim u_{xz} u_{yz}$. The efficiency of conversion (for fixed polarizations of the emitters) shows a sharp dependence on the magnitude of the external field (Fig. 12) and on its direction (see Ref. 35). Here the character of the interactions is described by the discussed mechanisms of the interactions. The extremum on the curve of Fig. 12 arises from the onset of detuning of the wave numbers $\Delta k = |k_1| - |k_2|$ as the field varies. In the experiment the increase in amplitude of the spin oscillations with decreasing field ($H < 0.5$ kOe) is restricted, in addition, by the increased damping of the sound.

Effects of acoustic convolution in $\alpha\text{-Fe}_2\text{O}_3$ have been observed also in the nonlinear interaction of surface magnetoelastic waves.^{36,37} The internal bilinear factor of the processes, i.e., the ratio of output electromagnetic power to the product of the acoustic powers of the interacting signals, in fields $H \approx 0.5$ kOe amounted to about -30 dB.m (-10 dB.m corresponds to 0.1 mW at the output for 1 mW at each of the two inputs).

In closing this section we note the experimental results in the field of nonlinear magnetoacoustics obtained with another high-temperature EPAF-FeBO_3 . Under transverse UHF pumping under conditions of antiferromagnetic resonance in iron borate, parametric instability of sound was

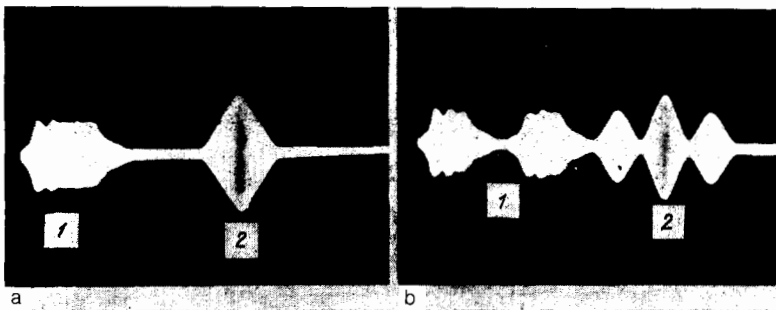


FIG. 11. Oscillograms of magnetoacoustic convolution signals in bulk waves in a crystal of $\alpha\text{-Fe}_2\text{O}_3$ ($L = 13$ mm).⁷⁰ 1—pulses at the input of the transducers (duration $1\mu\text{s}$), 2—pulses of the convolution at the receiving coil.

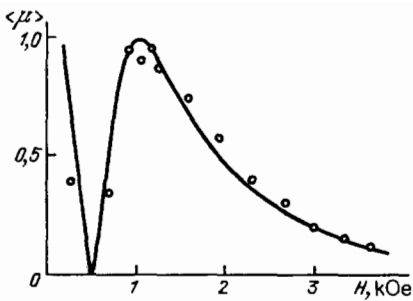


FIG. 12. Dependence of the amplitude of long-wavelength spin oscillations at the frequency $\omega = \omega_1 + \omega_2$ on the magnetic field intensity ($e_1 \parallel x \parallel H, e_2 \parallel y; L = 0.75 \text{ mm}$).³⁵

observed.^{38,39} The effect was treated theoretically in Ref. 40. Recently the excitation of a parametric acoustic echo by a high-frequency magnetic field was discovered in FeBO_3 .⁴¹ It was noted in an excellent review on iron borate,⁵ and this viewpoint cannot but be shared, that FeBO_3 , just like $\alpha\text{-Fe}_2\text{O}_3$, will serve in many regards as an extremely convenient object for studying numerous effects engendered by the very strong dynamic coupling of the elastic and magnetic subsystems of this EPAF.

It is pertinent to call attention to the fact that magnetoelastic interaction can substantially modify the acoustooptical properties of the crystals being discussed. Oscillations of the magnetic moments in the field of a sound wave lead to modulation of the magneto-optical birefringence (Cotton-Mouton effect) by forming specific "effective" acoustooptical parameters of the crystal that depend on the magnetic field. Such an acoustomagneto-optical modulation has been observed⁴² in $\alpha\text{-Fe}_2\text{O}_3$ in the near infrared range, where hematite is optically transparent. We can naturally expect to observe an analogous effect in FeBO_3 caused by the strong Faraday rotation of the plane of polarization of light and by the magnetoelastic interaction, including also the visible optical range ($\lambda \approx 0.5 \mu\text{m}$) where iron borate has a transparency window.

6. ACOUSTIC NONLINEARITY NEAR A SPIN REORIENTATION

Favorable conditions for forming a giant magnetoacoustic nonlinearity are realized in the vicinity of the magnetic orientational phase transitions approach to which gives rise to an anomalous growth in the magnon-phonon coupling owing to a decrease in the activation energy of one of the branches of the magnon spectrum.

The orientational transition in $\alpha\text{-Fe}_2\text{O}_3$ at the Morin point $T_M = 262 \text{ K}$ (see Ref. 4), which is caused by sign reversal of the uniaxial anisotropy, is apparently a first-order transition and essentially is not manifested in acoustic nonlinearity. According to the experimental data,⁴³ the antiferromagnetic branch of the spin waves responsible for this transition, although it softens at T_M , yet has an activation energy that still remains very high. Hence the coupling of sound with the waves of the antiferromagnetic branch is manifested weakly at the Morin point.⁴⁴ The situation might differ if one could stabilize one of the phases while approaching the point of lability with respect to the magnetic field—at this point the mode responsible for the transition "softens" most strongly.

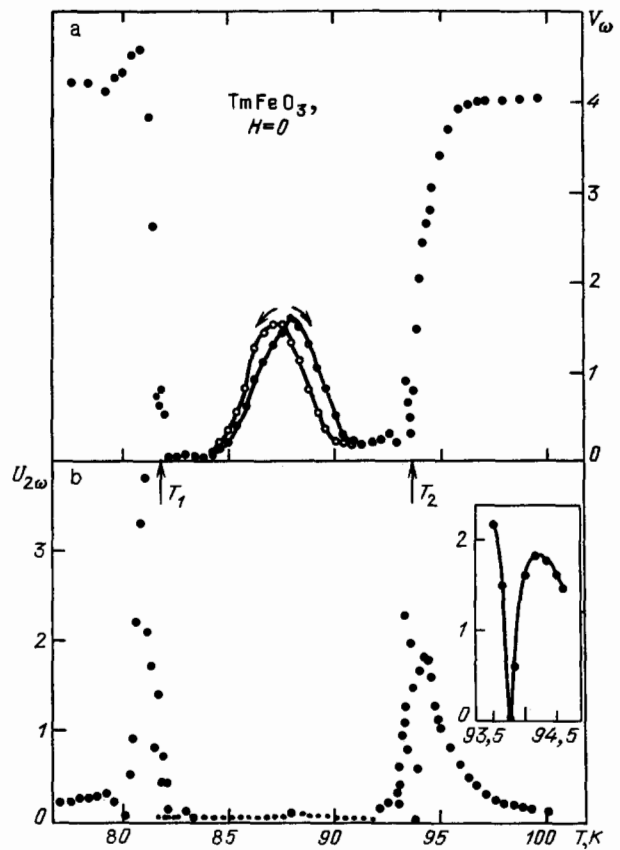


FIG. 13. Temperature dependence of the amplitudes of the first and second harmonics of sound at the output of a TmFeO_3 crystal near the spin-reorientation points T_1 and T_2 .⁴⁵

Experimentally the appearance of strong acoustic nonlinearity near an orientational phase transition (second-order!) has been demonstrated by observing an effect of generation of the second acoustic harmonic in the orthoferrite TmFeO_3 .⁴⁵ The TmFeO_3 crystal has an orthorhombic structure (the b axis is the "hard axis" for the magnetic moments of the sublattices), and the temperature of antiferromagnet-

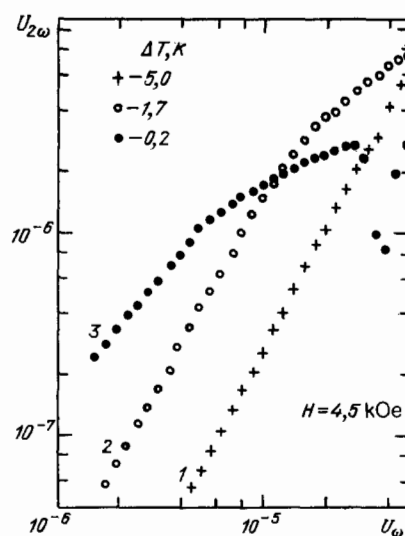


FIG. 14. Dependence of the amplitude of the second acoustic harmonic on the amplitude of the pump wave in TmFeO_3 ($\Delta T = T - T_1$).⁴⁵

ic ordering is $T_N = 630$ K. In the absence of an external magnetic field, changing temperature leads to reorientation of the spins from the a axis at $T \gg T_1 = 94$ K to the c axis at $T \ll T_2 = 82$ K. At $T_1 < T < T_2$ the vector \mathbf{l} rotates smoothly in the ac plane from the one axis to the other. The temperatures T_1 and T_2 are second-order orientational-transition points, near which the activation energy of the spin-wave modes is depressed (the mode becomes "soft"), as is confirmed experimentally by measuring the antiferromagnetic resonance frequency.⁴⁶ In the vicinity of the temperatures T_1 and T_2 a sharp increase has been observed in the efficiency of generation of the second acoustic harmonic (Figs. 13, 14). With increasing power of the pump wave, the output of the second harmonic is saturated and even declines owing to conversion of the energy of the incident wave, not only into the second harmonic, but also into a multitude of higher harmonics.

7. ON THE QUANTUM THEORY OF NONLINEAR INTERACTIONS OF COUPLED EXCITATIONS

The interaction of elementary excitations determines many thermodynamic and kinetic properties of crystals. As a rule, description of these properties requires one to apply quantum-statistical methods. The coupling of excitations gives shape to the effective nonlinear interactions, whose amplitudes can have an anomalously large magnitude and unusual dispersion properties. The selection rules for such interactions are often controlled by the external conditions, e.g., the orientation of the external field with respect to the crystallographic axes. All this introduces certain specifics into a number of phenomena that arise in crystals in the presence of coupling of subsystems.

The concept of the effective nonlinearity as being the nonlinearity of mixed elementary excitations is the basis for constructing its quantum theory.⁴⁷⁻⁴⁹ In a second-quantization scheme the transition to a representation of mixed modes is performed by diagonalizing the bilinear component of the Hamiltonian operator taking into account the coupling of the subsystems.^{9,47} This has the form

$$\begin{aligned} \hat{H}^{(2)} &= \sum_{\mathbf{k}, S} \{ \omega_{S\mathbf{k}} b_{S\mathbf{k}}^+ b_{S\mathbf{k}} + \omega_{l\mathbf{k}} c_{\mathbf{k}}^+ c_{\mathbf{k}} + (G_{S\mathbf{k}} b_{S\mathbf{k}}^+ c_{\mathbf{k}} + \text{H.c.}) \} \\ &= \sum_{\lambda=0}^3 \Omega_{\lambda\mathbf{k}} d_{\lambda\mathbf{k}}^+ d_{\lambda\mathbf{k}}. \end{aligned} \quad (31)$$

Here $b_{S\mathbf{k}}^+, b_{S\mathbf{k}}, c_{\mathbf{k}}^+, c_{\mathbf{k}}$ are the operators for creation and annihilation of phonons and magnons, and we have $G_{S\mathbf{k}} = \zeta_{S\mathbf{k}} (\omega_{S\mathbf{k}} \omega_{l\mathbf{k}})^{1/2}$. The operators for creation and annihilation of mixed excitations $d_{\lambda\mathbf{k}}^+$ and $d_{\lambda\mathbf{k}}$ are connected to the operators for the "pure" excitations by the unitary transformation:

$$c_{\mathbf{k}}^+ \pm c_{-\mathbf{k}} = \sum_{\lambda=0}^3 P_{\lambda\mathbf{k}} (d_{\lambda\mathbf{k}}^+ \pm d_{\lambda, -\mathbf{k}}), \quad (32)$$

$$b_{S\mathbf{k}} + b_{S, -\mathbf{k}}^+ = \sum_{\lambda=0}^3 R_{\lambda\mathbf{k}} (d_{\lambda\mathbf{k}}^+ + d_{\lambda, -\mathbf{k}}), \quad (33)$$

Here $P_{\lambda\mathbf{k}}$ and $R_{\lambda\mathbf{k}}$ are the transformation coefficients given in Ref. 47. Far from the intersection point of the "pure" spectra, the coupling of the terms with $\lambda = 1, 2, 3$ with the operators $c_{\mathbf{k}}^+$ and $c_{-\mathbf{k}}$ in Eq. (32), which is the quantum analog of Eq. (15), governs the nonresonance (virtual) excitation of magnons by quasiphonons. Therefore every nonlin-

ear process in the system of magnons is also a source of nonlinearity in the system of quasiphonons. Thus, an interaction of the type of (20) with participation of one phonon and two magnons studied phenomenologically is described by a contribution to the Hamiltonian having the form⁴⁷

$$\begin{aligned} \mathcal{H}^{(3)} &= N^{-1/2} \sum_{\mathbf{k}, \mathbf{q}} \Psi_{m\text{-ph}}^{(3)}(\mathbf{k}, \mathbf{q}) (b_{p\mathbf{k}} + b_{p, -\mathbf{k}}^+ \\ &\quad \times (c_{\mathbf{q}}^+ + c_{-\mathbf{q}}) (c_{-\mathbf{k}-\mathbf{q}}^+ + c_{\mathbf{k}+\mathbf{q}}). \end{aligned} \quad (34)$$

When we take account of the transformation (32), (33), this interaction is the source of three-particle processes in the system of quasiphonons:

$$\begin{aligned} \Delta \mathcal{H}^{(3)} &= N^{-1/2} \\ &\quad \times \sum_{\substack{\mathbf{k}, \mathbf{q} \\ l, \lambda, \nu}} \Psi_{l\lambda\nu}^{(3)}(\mathbf{k}, \mathbf{q}) (d_{\lambda\mathbf{k}}^+ + d_{\lambda, -\mathbf{k}}) (d_{\nu\mathbf{q}}^+ + d_{\nu, -\mathbf{q}}) \\ &\quad \times (d_{l(\mathbf{k}+\mathbf{q})} + d_{l(-\mathbf{k}-\mathbf{q})}^+). \end{aligned} \quad (35)$$

Here l, λ , and ν are the polarization indices of the quasiphonons, while the amplitude $\Psi_{l\lambda\nu}^{(3)}$ of the interaction is expressed in terms of the parameters of the quasiphonons and the effective elastic moduli, just as in ordinary lattice dynamics:

$$\begin{aligned} \Psi_{l\lambda\nu}^{(3)}(\mathbf{k}, \mathbf{q}) &= -\frac{1}{2^{3/2}} \left(\frac{\Omega_{\lambda\mathbf{k}} \Omega_{\nu\mathbf{q}} \Omega_{l(\mathbf{k}+\mathbf{q})}}{M_v^3 V_\lambda^2 V_\nu^2 V_l^2} \right) \\ &\quad \times \frac{J_0^2}{\omega_{l\mathbf{k}}^2 \omega_{l\mathbf{q}}^2} (\hat{\beta}_2 \hat{u}_{\lambda\mathbf{k}}) (\hat{\beta}_2 \hat{u}_{\nu\mathbf{q}}) (\hat{\beta}_1 \hat{u}_{l, \mathbf{k}+\mathbf{q}}). \end{aligned} \quad (36)$$

Here J_0 is the exchange energy; $V_\lambda = \Omega_{\lambda\mathbf{k}}/k$; $\hat{\beta}_{1,2} = \hat{B}_{1,2} v_0$; and v_0 and M_v are the volume and mass of the unit cell.

We can make the construction perspicuous by using the graphic representation for the vertex parts of the Feynman diagrams (Fig. 15). The diagram of Fig. 15a illustrates the interaction (34). The straight and wavy lines correspond to magnons and phonons. We can conveniently treat the transformation to the representation of the coupled waves, with formation of an effective vertex of interaction of quasiphonons (which corresponds to the double line), as the result of joining the phonon and the magnon lines. This merger is put into correspondence with the factor $(G_{S\mathbf{k}}/\omega_{l\mathbf{k}})$ in the analytic expression for the vertex with subsequent replacement of the phonon parameters (frequencies and polarizations) by the quasiphonon parameters. The description of any interaction of quasiphonons mediated by spin interactions is constructed analogously. The construction of the amplitude of the interaction of four quasiphonons corresponding to the effective fourth-order anharmonicity of (23) is illustrated in Fig. 15b.

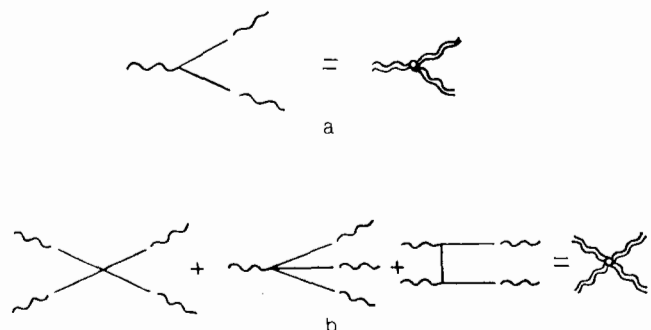


FIG. 15. Diagrams for vertices arising from effective anharmonicity of third⁴⁷ (a) and fourth²⁵ (b) orders.

We note that the discussed mechanisms of effective nonlinearity are not specifically of a quantum type, whereas the processes of interaction of quasiparticles caused by them, including those with participation of thermal excitations, can be of doubly quantum character, as happens in relaxation-kinetic phenomena. Taking account of the quantum-statistical properties of the spin-phonon system is necessary in describing the observable temperature and field dependences of the macroscopic effective elastic moduli themselves. To solve this problem as applied to a broad temperature range ($T \lesssim T_N$), a quantum theory has been proposed,^{48,49} based on the diagram technique for spin operators.⁶⁵⁻⁶⁷

A specific spatial dispersion of the interaction amplitudes (i.e., their dependence on k) caused by the dispersion of magnons is characteristic for effective anharmonicity. Dispersion restricts the phase volume of the interacting excitations to the region of small wave vectors $k_m \lesssim \omega_0/v_m$, since phonons with wave vectors of the order of the Debye value practically do not interact linearly with magnons ($\xi_{k-k_D} \rightarrow 0$). In this regard the effective anharmonicity of the elastic subsystem, which is giant in the long-wavelength region of the spectrum, is weak in the short-wavelength region and hence gives rise to relatively small energy losses of acoustic waves in processes of their scattering by short-wavelength (thermal) excitations.

The contribution of effective anharmonicity to the damping γ_k of sound is determined by the relationship⁴⁷

$$\frac{\gamma_k}{\Omega_k} \sim \frac{TT_N\beta^6}{\omega_{f0}^5 (Mv^2)^3}.$$

For hematite an estimate of the acoustic Q -factor $Q \equiv \Omega_k / 2\gamma_k$ yields $Q \sim 10^5 - 10^6$ for $k \ll k_m$. Here it is pertinent to note that the experimentally measurable acoustic losses in crystals of α -Fe₂O₃ are substantially higher²⁵ (Fig. 16). Apparently this is explained by the defect content of real crystals, which corresponds to the results of comparing the losses upon passage of sound through a specimen of α -Fe₂O₃ and relaxation times of the sonic field in experiments on reversal of the wave front of sound.³⁴ We should note that crystals of hematite containing an admixture of Al³⁺, which is isomorphous to trivalent iron, have a relatively higher Q -

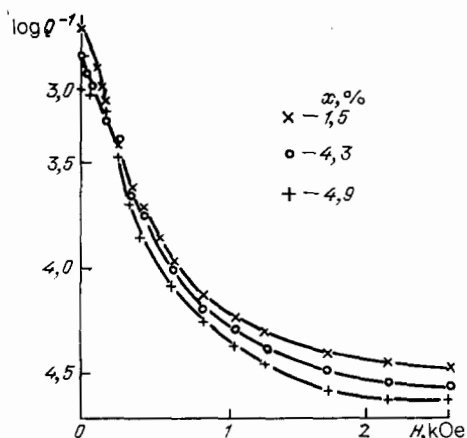


FIG. 16. Field dependence of the damping of magnetoelastic vibrations at the frequency 0.5 MHz in crystals of α -(Fe_{1-x}Al_x)₂O₃.²⁵

factor, owing to the decreased concentration of Fe²⁺ ions usually present in hematite in an amount of about 1%.⁶⁸

8. OUTSIDE THE ANHARMONIC APPROXIMATIONS

The arguments presented in Sec. 1 imply that, for magnetics having a strong enough magnon-phonon coupling ($\xi \sim 1$), the region of applicability of anharmonic expansions is limited to elastic deformations close in magnitude to the deformations of spontaneous magnetostriction. Such deformations are usually far from the limits for breakdown of real crystals and are relatively easily attained under the conditions of acoustic experimentation. In this regard it is of interest to study magnetoelastic excitations whose description lies outside the framework of anharmonic approximations and which involves the need for exact solution of strongly nonlinear systems of the dynamic equations (11) and (12). Under certain conditions the nonlinearity and dispersion introduced by the spin system into the magnetoelastic excitations can compensate one another. Consequently the possibility arises of formation of isolated coupled magnetoelastic waves—magnetoacoustic solitons.⁷¹ Such waves as applied to EPAFs were first studied in Ref. 50. Their different modifications, problems of stability, and the character of evolution of soliton solutions have been studied in Refs. 51-54.

We shall analyze the conditions of formation of magnetoacoustic solitons by using Eq. (7) with the example of waves propagating in rhombohedral EPAFs along the trigonal axis. If the wave is a steady-state one, i.e., $U = U(\xi)$ and $\varphi = \varphi(\xi)$, where $\xi \equiv z - Vt$, then we can eliminate the dynamic deformations from the system of equations (11), (12) and reduce it to the "double sine-Gordon" steady-state equation:

$$m_p \frac{\partial^2 \varphi}{\partial \xi^2} = A \sin \varphi + \frac{1}{2} D \sin 2\varphi. \quad (37)$$

Here we have

$$m_p \equiv \gamma^{-2} (v_m^2 - V^2), \quad A = HH_D,$$

$$D = \gamma^{-2} \left(\omega_{f0}^2 \frac{V_{st}^2 - V^2}{v_{st}^2 - V^2} - HH_D \gamma^2 \right),$$

$V_{st} \equiv v_{st} (1 - \xi^2)^{1/2}$ is the velocity of the soundlike wave. Following Ref. 55, we can easily establish the intervals of velocities V of waves corresponding to soliton solutions and the qualitative features of the motion of the magnetic moments by using the evident analogy of Eq. (30) with the equation of motion of a particle of mass m_p and momentum $p = m_p \partial \varphi / \partial \xi$ in a force field having the potential

$$\tilde{f}(\varphi) = A (\cos \varphi - 1) + \frac{1}{4} D (\cos 2\varphi - 1).$$

In crystals of EPAFs having a high Neel temperature (α -Fe₂O₃, FeBO₃), for which $v_m > v_{st}$, the attainable velocities of motion of solitons in the z direction must satisfy the conditions: $V^2 < V_{st}^2$ or $v_m^2 > V^2 > v_{st}^2$. In these cases the effective potential has the characteristic form shown in Fig. 17a. An isolated wave on the background of the equilibrium state of the crystal ($\varphi \equiv 0$) corresponds to motion of the "particle" in the potential well $F(\varphi)$ from the point $(\varphi|_{\xi \rightarrow -\infty} = 0$ for $p|_{\xi \rightarrow -\infty} = 0)$ to the point $(\varphi|_{\xi \rightarrow +\infty} = 2\pi$ for $p|_{\xi \rightarrow +\infty} = 0)$, i.e., continuous rotation of the magnetic moment in the wave by the angle 2π . A solution of the given type

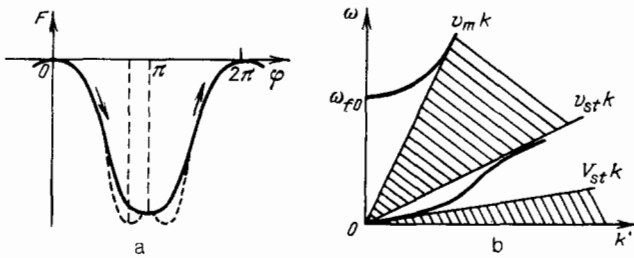


FIG. 17. a—Dependence of the effective potential on the angle φ of deviation of the vector \mathbf{e} from the equilibrium direction.²⁵ b—Regions of existence for the velocities of solitons in a high-temperature EPAF ($v_m > v_{st}$).²⁵

amounts to the well known “ 2π kink” of the “double sine-Gordon” equation⁵⁰:

$$\operatorname{tg} \frac{\varphi}{2} = \left(\frac{D+A}{A} \right)^{1/2} \left(\operatorname{sh} \frac{\xi}{\xi_0} \right)^{-1}. \quad (38)$$

Here the characteristic dimension of a soliton is $\xi_0 = [m_p / (D+A)]^{1/2}$. For the α - Fe_2O_3 crystal with $H \approx 0.5$ kOe and $V \ll V_{st}$, the magnitude of ξ_0 is $\sim 10^{-3} - 10^{-4}$ cm, while the maximum deformations in the wave are of the order of 10^{-5} . We should pay attention to the fact that the velocities of solitons take on values that do not coincide with the phase velocities of linear magnetoelastic waves. In the ωk plane each value $v_{ph} \equiv \omega/k$ of the harmonic wave can be put into correspondence with a straight line passing through the coordinate origin with a slope equal to $\tan \alpha = v_{ph}$. The regions in which these straight lines can lie are left uncross-hatched in Fig. 17b. In turn, the crosshatched regions correspond to the attainable velocities of solitons ($V = \tan \alpha$). Such a segmentation of the ωk plane is valid for any directions of propagation of magnetoelastic waves, if we do not take into account relaxation, which amounts to a generalized result of the action of the nonlinear interactions not taken into account in (11), (12).

In low-temperature EPAFs for which $v_m < v_{st}$ (MnCO_3 , CoCO_3), solitons correspond to velocities $v_{st} > V > v_m$ or $V < v_m$ (Fig. 18b). In the former case the solitons also have the form of a 2π kink, and in the latter case their structure proves qualitatively different. The characteristic form of the effective potential of a “particle” of mass $|m_p|$ for the range of near-sonic velocities $v_{st} > V > v_m$ is shown in Fig. 18a. A soliton corresponds to motion of the “particle” from the point $\varphi = 0$ (for $p = 0$) to the point φ_{max} with subsequent return to the point $\varphi = 0$. Here the solution

of Eq. (30) has the form⁵⁰

$$\operatorname{tg} \frac{\varphi}{2} = \left(\frac{|D+A|}{A} \right)^{1/2} \left(\operatorname{ch} \frac{\xi}{\xi_0} \right)^{-1}. \quad (39)$$

In contrast to a 2π kink, the given type of solitons can be realized for any deviations from equilibrium ($\varphi_{max} \ll 1$). In this case the result goes over into the known soliton solution of the modified Korteweg-de Vries equation (see Ref. 55). From the experimental standpoint it seems interesting to estimate the time τ during which such a soliton evolves from the initial steplike magnetoelastic perturbation moving with the velocity V_{st} .⁵¹ For the typical low-temperature EPAF MnCO_3 we find $\tau = \xi_0 / |V - V_{st}| \sim 10^{-6}$, and the length of specimen necessary for a pulse experiment does not exceed 1 cm. Estimates of τ for an elastic soliton with a nonlinear elastic lattice or for a magnetoelastic soliton in a ferromagnetic having a moderate magnetoelastic interaction yield $\tau \sim 0.1$ s, thus demonstrating the advantages of nonconductive EPAFs for direct observation of isolated magnetoelastic waves. We must note that soliton solutions of the original system (11), (12) for magnetoelastic waves of small amplitude with near-sonic velocities also exist in high-temperature EPAFs, but for other directions of propagation.⁵¹ However, in these crystals such excitations prove to be unstable with respect to transverse perturbations of their front.^{52,54} One of the variants of the development of this instability turns out to be self-focusing of the magnetoelastic excitations.⁵² Its physical cause is the decrease in velocity of the excitation with increase in its amplitude, which causes an accumulating deflection of the wave front in a direction opposite to the direction of propagation. A detailed analysis of the initial distributions of the amplitude from which the self-focusing wave is formed has been performed in Ref. 53.

The evident qualitative differences between solitons of the types (38) and (39) (see Figs. 17 and 18) allow a certain topological treatment. The solitons of (38) have a nonzero topological charge ($1/2\pi \oint \nabla \varphi \cdot d\mathbf{l} = 1$), where the integration is performed over a contour closed at infinity penetrating the base plane. By analogy with the vortex states in extended Josephson structures, such excitations can be classified as vortex excitations. For the solitons of (39) the topological charge is zero.

In the case of the excitations of (39) a crystal with fixed boundary conditions ($\varphi|_{z=\pm L} = 0$) can be converted by continuous transformation to the equilibrium state. Under the same conditions for excitations of the form of (38) the transition to equilibrium involves overcoming a finite energy barrier due to the exchange interaction. Accordingly the so-

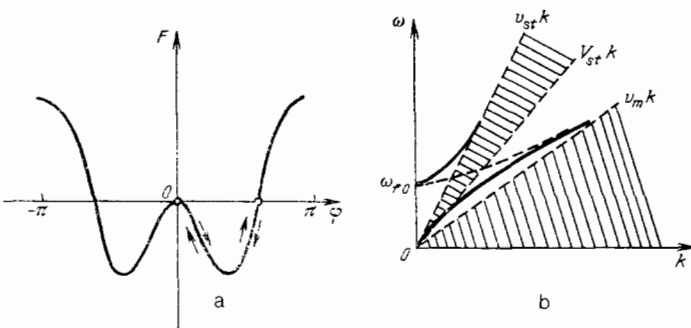


FIG. 18. a—Dependence of the effective potential on the angle φ of deviation of the vector \mathbf{e} from the equilibrium direction.²⁵ b—Regions of existence for the velocities of solitons in a low-temperature EPAF ($v_m < v_{st}$).²⁵

litons of (38) are topologically stable—in contrast to the solitons of (39). A calculation of the spectra of their localized excitations²⁵ shows that the given type of solitons is stable not only topologically, but also dynamically, which allows us to expect a possible experimental observation. For example, it seems possible to create a vortex soliton excitation by continuous rotation of the intensity vectors of an external magnetic field near the opposite boundaries of the specimen ($z = \pm L$) about one another by the angle 2π .

We note that strongly nonlinear spin excitations are substantially magnetoelastic even in crystals with relatively weak magnon-phonon coupling if their velocity of propagation is close to resonance with the sound velocity. In particular, such a situation arises in the orthoferrites in the motion of domain boundaries with near-sonic velocities.^{56,57}

CONCLUSION

As we see it, the ideas presented in the review on the effective nonlinearity of mixed modes are highly general in character. Not only magnetoelastic, but also electron-nuclear-spin and electron-nuclear-magnetoelastic waves, ferroelectromagnetic, and ferroelectric-magnetoelastic waves, polaritons, and other types of coupled oscillations can play the role of mixed excitations. Nonlinear processes in such systems have been intensively studied in recent years^{58–63}—mainly theoretically. An expansion of the experimental studies of strong effective interactions in coupled systems would facilitate the further development of our views of the mechanisms of formation of the dynamical properties of solids and their functional potentialities in technical applications.

¹Hereinafter (for brevity of notation) the symbol $(\hat{B})^n$ denotes the $2n$ -th rank tensor $B_{ij}B_{kl}\dots B_{pq}$.

²Analogous results have also been obtained in Refs. 22 and 23.

³Hereinafter we use the Vogt notation: $xx-1$; $yy-2$; $zz-3$; $yz-4$; $xz-5$; $xy-6$.

¹L. K. Zarembo and V. A. Krasil'nikov, *Usp. Fiz. Nauk* **102**, 549 (1970) [*Sov. Phys. Usp.* **13**, 778 (1971)].

²L. I. Mandel'shtam, *Lectures on Vibration Theory* (in Russian), Nauka, M., 1972, p. 214.

³V. I. Ozhogin, *Proc. 3rd Intern. School of Condensed Matter Physics*, ed. M. Borissov, World Scientific, Singapore, 1984, p. 434.

⁴I. S. Jacobs, R. A. Beyerlein, S. Foner, and J. P. Remeika, *J. Magn. Mater.* **1**, 193 (1971).

⁵R. Dichl, W. Jantz, B. I. Nolang, and W. Wetzling, *Current Topics in Materials Science*, ed. E. Kaldis, **11**, 242 (1986).

⁶M. H. Seavey, *Solid State Commun.* **10**, 219 (1972).

⁷a) V. I. Ozhogin and P. P. Maksimenkov, *Digests of Intermag Conference, Kyoto, 1972–49–4*; b) *IEEE Trans. Magn. MAG-8*, 130 (1972); c) *Zh. Eksp. Teor. Fiz.* **65**, 657 (1973) [*Sov. Phys. JETP* **38**, 324 (1974)].

⁸R. Z. Levitin, A. S. Pachomov, and V. A. Schurov, *Phys. Lett. A* **27**, 603 (1968).

⁹M. A. Savchenko, *Fiz. Tverd. Tela (Leningrad)* **6**, 864 (1964) [*Sov. Phys. Solid State* **6**, 666 (1964)].

¹⁰A. S. Borovik-Romanov and E. G. Rudashevskii, *Zh. Eksp. Teor. Fiz.* **47**, 2095 (1964) [*Sov. Phys. JETP* **20**, 1407 (1965)].

¹¹E. A. Turov and V. G. Shavrov, *Fiz. Tverd. Tela (Leningrad)* **7**, 217 (1965) [*Sov. Phys. Solid State* **7**, 166 (1965)].

¹²E. A. Turov and V. G. Shavrov, *Usp. Fiz. Nauk* **140**, 429 (1983) [*Sov. Phys. Usp.* **26**, 593 (1983)].

¹³V. I. Ozhogin and V. L. Preobrazhenskii, *Zh. Eksp. Teor. Fiz.* **73**, 988 (1977) [*Sov. Phys. JETP* **46**, 523 (1977)].

¹⁴V. G. Bar'yakhtar, B. A. Ivanov, and A. L. Sukstanskii, *Zh. Eksp. Teor. Fiz.* **78**, 1509 (1980) [*Sov. Phys. JETP* **51**, 757 (1980)].

¹⁵A. F. Andreev and V. I. Marchenko, *Usp. Fiz. Nauk* **130**, 39 (1980) [*Sov. Phys. Usp.* **23**, 21 (1980)].

¹⁶L. V. Velikov, S. V. Mironov, and E. G. Rudashevskii, *Zh. Eksp. Teor. Fiz.* **75**, 1110 (1987) [*Sov. Phys. JETP* **48**, 559 (1978)].

¹⁷V. I. Ozhogin, *IEEE Trans. Magn. MAG-12*, 19 (1976); *Izv. Akad.*

Nauk SSSR Ser. Fiz. **42**, 1625 (1978). [*Bull. Acad. Sci. USSR, Phys. Ser.* **42** (8), 48 (1978)].

¹⁸I. E. Dikshstein, V. V. Tarasenko, and V. G. Shavrov, *Zh. Eksp. Teor. Fiz.* **67**, 816 (1974) [*Sov. Phys. JETP* **40**, 404 (1975)].

¹⁹V. V. Berezhnov, N. N. Evtikhiev, V. L. Preobrazhenskii, and N. A. Ékonomov, *Radiotekh. Elektron.* **28**, 376 (1983) [*Radio Eng. Electron. (USSR)* **28** (1983)].

²⁰R. I. Kukhtin, V. L. Preobrazhenskii, and N. A. Ékonomov, *Fiz. Tverd. Tela (Leningrad)* **26**, 884 (1984) [*Sov. Phys. Solid State* **26**, 536 (1984)].

²¹V. V. Berezhnov, N. N. Evtikhiev, V. L. Preobrazhenskii, and N. A. Ékonomov, *Akust. Zh.* **26**, 328 (1980) [*Sov. Phys. Acoust.* **26**, 180 (1980)].

²²A. I. Alekseev, V. A. Ermolov, V. S. Bondarenko, and N. F. Naumenko, *Fiz. Tverd. Tela (Leningrad)* **26**, 2443 (1984) [*Sov. Phys. Solid State* **26**, 1480 (1984)].

²³T. A. Mamatova and V. G. Prokoshev, *Vestn. Mosk. Univ. Fiz. Astron.* **26**, 49 (1985).

²⁴V. L. Preobrazhenskii, M. A. Savchenko, and N. A. Ékonomov, *Pis'ma Zh. Eksp. Teor. Fiz.* **28**, 93 (1978) [*JETP Lett.* **28**, 87 (1978)].

²⁵V. L. Preobrazhenskii, *Magnetoacoustics of High-Temperature Antiferromagnetic Dielectrics with "Easy-Plane" Type Anisotropy* (in Russian): Abstract of dissertation for doctorate in physical-mathematical sciences, Institute of Radio Engineering, Electronics, and Automation, Moscow, 1986.

²⁶V. V. Berezhnov, N. N. Evtikhiev, V. L. Preobrazhenskii, and N. A. Ékonomov, *Fiz. Tverd. Tela (Leningrad)* **25**, 1870 (1982) [*Sov. Phys. Solid State* **25**, 1079 (1982)].

²⁷V. I. Ozhogin, A. Yu. Lebedev, and A. Yu. Yakubovskii, *Pis'ma Zh. Eksp. Teor. Fiz.* **27**, 333 (1978) [*JETP Lett.* **27**, 313 (1978)].

²⁸V. A. Krasil'nikov, T. A. Mamatova, and V. G. Prokoshev, *Pis'ma Zh. Tekh. Fiz.* **10**, 1196 (1984) [*Sov. Tech. Phys. Lett.* **10**, 506 (1984)].

²⁹A. Yu. Lebedev, V. I. Ozhogin, and A. Yu. Yakubovskii, *Pis'ma Zh. Eksp. Teor. Fiz.* **34**, 22 (1981) [*JETP Lett.* **34**, 19 (1981)].

³⁰V. V. Berezhnov, V. L. Preobrazhenskii, N. A. Ékonomov, and D. É. Élyashev, *Abstracts of reports at the 16th All-Union Conference on Physics of Magnetic Phenomena, Tula, 1983*, p. 23.

³¹F. V. Bunkin, Yu. A. Kravtsov, and G. A. Lyakhov, *Usp. Fiz. Nauk* **149**, 391 (1986) [*Sov. Phys. Usp.* **29**, 607 (1986)].

³²N. N. Evtikhiev, V. L. Preobrazhenskii, M. A. Savchenko, and N. A. Ékonomov, *Vopr. Radioelektron. Ser. Obshchetekhn. No. 5*, 124 (1978).

³³R. L. Comstock and R. C. LeCraw, *Phys. Rev. Lett.* **10**, 219 (1963).

³⁴V. A. Krasil'nikov, T. A. Mamatova, and V. G. Prokoshev, *Fiz. Tverd. Tela (Leningrad)* **28**, 615 (1986) [*Sov. Phys. Solid State* **28**, 346 (1986)].

³⁵V. V. Berezhnov, N. N. Evtikhiev, V. L. Preobrazhenskii, and N. A. Ékonomov, *Akust. Zh.* **26**, 328 (1980) [*Sov. Phys. Acoust.* **26**, 180 (1980)].

³⁶M. K. Gubkin, T. A. Mamatova, and V. G. Prokoshev, *ibid.* **31**, 678 (1985) [*Sov. Phys. Acoust.* **31**, 410 (1985)].

³⁷V. A. Ermolov, A. I. Alekseev, and V. G. Pankratov, *Pis'ma Zh. Tekh. Fiz.* **11**, 377 (1985) [*Sov. Tech. Phys. Lett.* **11**, 156 (1985)].

³⁸W. Wetzling, W. Jantz, and C. E. Patton, *J. Appl. Phys.* **50**, 2030 (1979).

³⁹B. Ya. Koytuzhanskii and L. A. Prozorova, *Zh. Eksp. Teor. Fiz.* **83**, 1567 (1982) [*Sov. Phys. JETP* **56**, 903 (1982)].

⁴⁰V. S. Lutovinov and M. A. Savchenko, *Abstracts of reports at the All-Union Conference on the Physics of Magnetic Phenomena, Khar'kov, 1979*, p. 85.

⁴¹M. V. Petrov, A. P. Paugurt, I. V. Pleshakov, and A. V. Ivanov, *Pis'ma Zh. Tekh. Fiz.* **11**, 1204 (1985) [*Sov. Tech. Phys. Lett.* **11**, 498 (1985)].

⁴²N. N. Evtikhiev, V. V. Moshkin, V. L. Preobrazhenskii, and N. A. Ékonomov, *Pis'ma Zh. Eksp. Teor. Fiz.* **35**, 31 (1982) [*JETP Lett.* **35**, 38 (1982)].

⁴³V. I. Ozhogin and V. G. Shapiro, *Zh. Eksp. Teor. Fiz.* **55**, 1737 (1968) [*Sov. Phys. JETP* **28**, 915 (1969)].

⁴⁴N. N. Evtikhiev, V. L. Preobrazhenskii, V. N. Shumilov, and N. A. Ékonomov, *Abstracts of reports at the All-Union Conference on the Physics of Magnetic Phenomena, Perm', 1981, Part 1*, p. 63.

⁴⁵A. Yu. Lebedev, V. I. Ozhogin, and A. Yu. Yakubovskii, *Zh. Eksp. Teor. Fiz.* **85**, 1059 (1983) [*Sov. Phys. JETP* **58**, 616 (1983)].

⁴⁶R. C. LeCraw, R. Wolfe, E. M. Gyorgy, F. B. Hagedorn, J. C. Hensel, and J. P. Remeika, *J. Appl. Phys.* **39**, 101 (1968).

⁴⁷V. S. Lutovinov, V. L. Preobrazhenskii, and S. P. Semin, *Zh. Eksp. Teor. Fiz.* **74**, 1159 (1978) [*Sov. Phys. JETP* **47**, 609 (1978)].

⁴⁸L. V. Panina and V. L. Preobrazhenskii, *Fiz. Met. Metalloved.* **57**, No. 1, 39 (1984). [*Phys. Met. Metallogr. (USSR)* **57**, No. 1, 30 (1984)].

⁴⁹L. V. Panina, V. L. Preobrazhenskii, V. N. Shumilov, and N. A. Ékonomov, *Akust. Zh.* **30**, 566 (1984) [*Sov. Phys. Acoust.* **30**, 335 (1984)].

⁵⁰V. L. Preobrazhensky and M. A. Savchenko, *Proc. 20th Congress of AMPERE, Tallinn, 1978*, p. 410.

- ⁵¹V. I. Ozhogin and A. Yu. Lebedev, *J. Magn. Magn. Mater.* **15-18**, 617 (1980).
- ⁵²V. I. Ozhogin, D. Y. Manin, V. I. Petviashvili, and A. Yu. Lebedev, *IEEE Trans. Magn.* **MAG-19**, 1977 (1983).
- ⁵³V. D. Buchel'nikov and V. G. Shavrov, *Fiz. Tverd. Tela (Leningrad)* **25**, 90 (1983) [*Sov. Phys. Solid State* **25**, 49 (1983)].
- ⁵⁴S. K. Turitsyn and G. E. Fal'kovich, *Zh. Eksp. Teor. Fiz.* **89**, 258 (1985) [*Sov. Phys. JETP* **62**, 146 (1985)].
- ⁵⁵B. B. Kadomtsev, *Collective Phenomena in a Plasma* (in Russian), Nauka, M., 1976, p. 121.
- ⁵⁶A. K. Zvezdin and A. F. Popkov, *Fiz. Tverd. Tela (Leningrad)* **21**, 1334 (1979) [*Sov. Phys. Solid State* **21**, 771 (1979)].
- ⁵⁷V. G. Bar'yakhtar, B. A. Ivanov, and M. V. Chetkin, *Usp. Fiz. Nauk* **146**, 417 (1985) [*Sov. Phys. Usp.* **28**, 563 (1985)].
- ⁵⁸V. S. Lutovinov and V. L. Safonov, *Fiz. Tverd. Tela (Leningrad)* **21**, 2772 (1979) [*Sov. Phys. Solid State* **21**, 1594 (1979)].
- ⁵⁹M. A. Savchenko and V. P. Sobolev, Abstracts of reports at the All-Union Conference on the Physics of Magnetic Phenomena, Donetsk, 1985, p. 318.
- ⁶⁰M. A. Savchenko and M. A. Khabakhpashev, *Fiz. Tverd. Tela (Leningrad)* **18**, 2699 (1976); **20**, 1845 (1978) [*Sov. Phys. Solid State* **18**, 1573 (1976); **20**, 1065 (1978)].
- ⁶¹G. A. Farias and A. A. Maradudin, *Phys. Rev. B* **28**, 1870 (1983).
- ⁶²V. V. Men'shenin, I. F. Mirsaev, and G. G. Taluts, *Fiz. Met. Metalloved.* **56**, No. 6, 1078 (1983). [*Phys. Met. Metallogr. (USSR)* **56**, No. 6, 30 (1983)].
- ⁶³V. P. Lukomskii, *Fiz. Tverd. Tela (Leningrad)* **20**, 2797 (1978) [*Sov. Phys. Solid State* **20**, 1613 (1978)].
- ⁶⁴V. A. Murashov, A. V. Rozantsev, A. N. Sidorov, T. A. Zharinova, V. N. Shumilov, and V. V. Moshkin, *Tr. MKhTI*, No. 133, 21 (1984).
- ⁶⁵V. G. Vaks, A. I. Larkin, and S. A. Pikin, *Zh. Eksp. Teor. Fiz.* **53**, 1089 (1967) [*Sov. Phys. JETP* **26**, 647 (1968)].
- ⁶⁶E. M. Pikalev, M. A. Savchenko, and J. Solyom, *Zh. Eksp. Teor. Fiz.* **55**, 1404 (1968) [*Sov. Phys. JETP* **28**, 734 (1969)].
- ⁶⁷Yu. A. Izyumov, S. A. Kasan-Ogly, and Yu. N. Skryabin, *Field Methods in the Theory of Ferromagnetism* (in Russian), Nauka, M., 1984, p. 224.
- ⁶⁸V. A. Murashov, A. N. Sidorov, T. A. Zharinova, V. N. Surkov, and Yu. M. Mosin, Abstracts of reports at the 3rd All-Union Conference "Status and Perspectives of Development of Methods of Obtaining Single Crystals" (In Russian), Khar'kov, 1985, p. 86.
- ⁶⁹R. K. Bullough, P. J. Caudrey, and H. M. Gibbs, in: *Solitons*, eds. R. K. Bullough and P. J. Caudrey, Springer-Verlag, Berlin, 1980, p. 107 (Russ. transl., Mir, M., 1983, p. 122).
- ⁷⁰V. V. Berezhnov, *Vopr. Radioelektron. Ser. Obshchetechn.*, No. 11, 121 (1982).
- ⁷¹E. V. Volzhan, N. P. Giorgadze, and A. D. Pataraya, *Zh. Eksp. Teor. Fiz.* **70**, 1330 (1976) [*Sov. Phys. JETP* **43**, 693 (1976)].

Translated by M. V. King